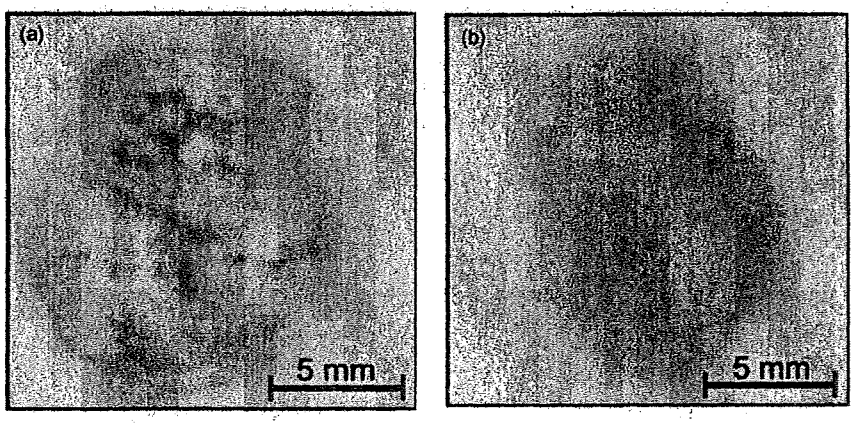

Fig. 5. Extravasation of Evans blue in LLC (a) and C26 tumors (b). Forty-eight hours after intravenous injection of Evans blue solution, tumors were excised and were snap-frozen. Cross-sections of tumor tissues were directly subjected to the observation under the microscope as described in Section 2. The result shown here is the representative one among three independent tumor sections per group.

amount of VEGF was secreted in C26 tumor compared with that of LLC tumor (Fig. 6c). From these results, it was suggested that the higher vascular permeability within C26 tumor (Fig. 5) would be ascribed to its higher secretion of VEGF within the tumor tissue. Mediators that would be substantially responsible for enhancing the secretion of VEGF in these tumor tissues remain unclear, but should be identified for the development of the more efficient cancer chemotherapy.

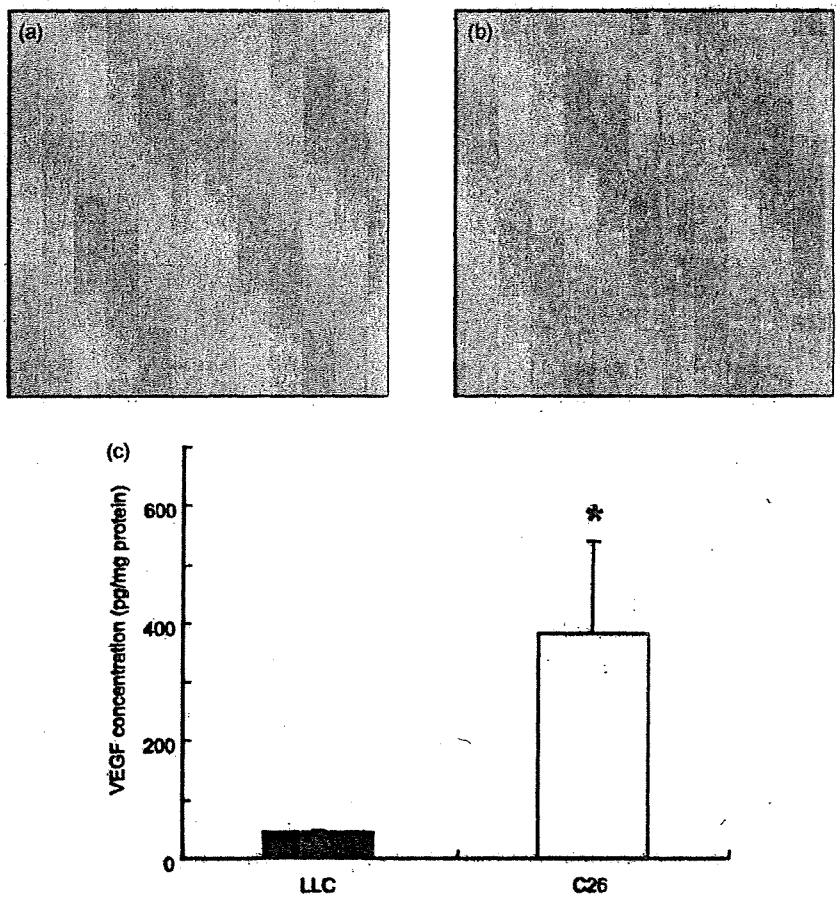

Fig. 6. Immunohistochemical staining of VEGF in LLC (a) and C26 tumors (b), and quantification of VEGF amount within the tumor tissue by ELISA (c). Tumor tissues were excised from mice when the tumor became 500 mm^3 in volume and were snap-frozen. Acetone-fixed 5-μm thick sections of tumor tissues were prepared and then AEC staining was performed for VEGF as described in Section 2. In parallel, tumor tissues were homogenized in lysis buffer containing 5% protease inhibitor cocktail and VEGF levels were quantified with commercially available ELISA kit. Results are expressed as the mean with the vertical bar showing S.D. of four independent experiments. *$p < 0.05$, compared with LLC.

The present study clearly demonstrated that besides the improvement of retention of liposomal DOX in plasma, the higher vascular permeability within tumor tissues would also be required for liposomal DOX to be taken up more efficiently by tumor cells, indicating that the permeability of vasculature within tumor tissues is a critical factor for EPR effect-based anti-tumor effect of liposomal DOX.

References

Amice, J., Dazord, L., Toujas, L., 1978. Impairment of inflammatory reactions in tumour-bearing mice as measured by Evans blue extravasation. Eur. J. Cancer 14, 1287–1289.

Clasen, R.A., Pandolfi, S., Hass, G.M., 1970. Vital staining, serum albumin and the blood-brain barrier. J. Neuropathol. Exp. Neurol. 29, 266–284.

Dreher, M.R., Liu, W., Michelich, C.R., Dewhirst, M.W., Yuan, F., Chilkoti, A., 2006. Tumor vascular permeability, accumulation, and penetration of macromolecular drug carriers. J. Natl. Cancer Inst. 98, 335–344.

Eghbali, M., Birnir, B., Gage, P.W., 2003. Conductance of $GABA_A$ channels activated by pentobarbitone in hippocampal neurons from newborn rats. J. Physiol. 552, 13–22.

Gabizon, A.A., 1995. Liposome circulation time and tumor targeting: Implications for cancer chemotherapy. Adv. Drug Del. 16, 285–294.

Gabizon, A.A., Chemla, M., Tzemach, D., Horowitz, A.T., Goren, D., 1996. Liposome longevity and stability in circulation: effects on the in vivo delivery to tumors and therapeutic efficacy of encapsulated anthracyclines. J. Drug Target. 3, 391–398.

Gabizon, A.A., Shmeeda, H., Zalipsky, S., 2006. Pros and cons of the liposome platform in cancer drug targeting. J. Liposome Res. 16, 175–183.

Graff, B.A., Bjornaes, I., Rofstad, E.K., 2000. Macromolecule uptake in human melanoma xenografts: relationships to blood supply, vascular density, microvessel permeability and extracellular volume fraction. Eur. J. Cancer 36, 1433–1440.

Graff, B.A., Bjonaes, I., Rofstad, E.K., 2001. Microvascular permeability of human melanoma xenografts to macromolecules: relationships to tumor volumetric growth rate, tumor angiogenesis and VEGF expression. Microvascular Res. 61, 187–198.

Haran, G., Cohen, R., Bar, L.K., Barenholz, Y., 1993. Transmembrane ammonium sulfate gradient in liposomes produce efficient and stable entrapment of amphipathic weak bases. Biochim. Biophys. Acta 1151, 201–215.

Heyes, J., Hall, K., Tailor, V., Lenz, R., MacLachlan, I., 2006. Synthesis and characterization of novel poly(ethylene glycol)-lipid conjugates suitable for use in drug delivery. J. Control. Release 112, 280–290.

Kliche, S., Waltenberger, J., 2001. VEGF receptor signaling and endothelial function. IUBMB Life 52, 61–66.

Kratzke, R.A., Kramer, B.S., 1996. Evaluation of in vitro chemosensitivity using human lung cancer cell lines. J. Cell Biochem. 24, 160–164.

Lee, E.S., Na, K., Bae, Y.H., 2005. Doxorubicin loaded pH-sensitive polymeric micelles for reversal of resistant MCF-7 tumor. J. Control. Release 103, 405–418.

Lim, J.G., Lee, H.Y., Yun, J.E., Kim, S.P., Park, J.W., Kim, S.S., Han, J., Park, M.J., Song, D.K., 2004. Taurine block of cloned ATP-sensitive K^+ channels with different sulfonylurea receptor subunits expressed in *Xenopus laevis* oocytes. Biochem. Pharmacol. 68, 901–910.

Maeda, H., Wu, J., Sawa, T., Matsumura, Y., Hori, K., 2000. Tumor vascular permeability and the EPR effect in macromolecular therapeutics: a review. J. Control. Release 65, 271–284.

Mayer, L.D., Tai, L.C., Ko, D.S., Masin, D., Ginsberg, R.S., Cullis, P.R., Bally, M.B., 1989. Influence of vesicle size, lipid composition, and drug-to-lipid ratio on the biological activity of liposomal doxorubicin in mice. Cancer Res. 49, 5922–5930.

Mosmann, T., 1983. Rapid colorimetric assay for cellular growth and survival: application to proliferation and cytotoxicity assays. J. Immunol. Methods 65, 55–63.

Nakamura, R., Saikawa, Y., Kubota, T., Kumagai, A., Kiyota, T., Ohashi, M., Yoshida, M., Otani, Y., Kumai, K., Kitajima, M., 2006. Role of the MTT chemosensitivity test in the prognosis of gastric cancer patients after postoperative adjuvant chemotherapy. Anticancer Res. 26, 1433–1437.

Northfelt, D.W., Dezube, B.J., Thommes, J.A., Miller, B.J., Fischl, M.A., Friedman-Kien, A., Kaplan, L.D., Mond, C.D., Mamelok, R.D., Henry, D.H., 1998. Pegylated-liposomal doxorubicin versus doxorubicin, bleomycin, and vincristine in the treatment of AIDS-related Kaposi's sarcoma: results of a randomized phase III clinical trial. J. Clin. Oncol. 16, 2445–2451.

Roberts, W.G., Hasan, T., 1993. Tumor-secreted vascular permeability factor/vascular endothelial growth factor influences photosensitizer uptake. Cancer Res. 53, 153–157.

Schmidt, P.G., Adler-Moore, J.P., Forssen, E.A., Proffit, R.T., 1998. Unilamellar liposomes for anticancer and antifungal therapy. In: Lasic, D.D., Papahadjopoulos, D. (Eds.), Medical Applications of Liposomes. Elsevier Science BV, New York, pp. 703–731.

Shaw, G.L., Gazdar, A.F., Phelps, R., Steinberg, S.M., Linnoila, R.I., Johnson, B.E., Oie, H.K., Russell, E.K., Ghosh, B.C., Pass, H.I., Minna, J.D., Mulshine, J.L., Ihde, D.C., 1996. Correlation of in vitro drug sensitivity testing results with response to chemotherapy and survival: comparison of non-small cell lung cancer and small cell lung cancer. J. Cell Biochem. 24, 173–185.

Smit, E.F., de Vries, E.G., Timmer-Bosscha, H., de Leij, L.F., Oosterhuis, J.W., Scheper, R.J., Weening, J.J., Postmus, P.E., Mulder, N.H., 1992. In vitro response of human small-cell lung-cancer cell lines to chemotherapeutic drugs; no correlation with clinical data. Int. J. Cancer 51, 72–78.

Tanaka, S., Akaike, T., Wu, J., Fang, J., Sawa, T., Ogawa, M., Beppu, T., Maeda, H., 2003. Modulation of tumor-selective vascular blood flow and extravasation by the stable prostaglandin 12 analogue beraprost sodium. J. Drug Target 11, 45–52.

Tonn, J.C., Schachenmayr, W., Kraemer, H.P., 1994. In vitro chemosensitivity test of malignant gliomas: clinical relevance of test results independent of adjuvant chemotherapy. Anticancer Res. 14, 1371–1375.

Unezaki, S., Maruyama, K., Hosoda, J.I., Nagae, I., Koyanagi, Y., Nakata, M., Ishida, O., Iwatsuru, M., Tsuchiya, S., 1996. Direct measurement of the extravasation of polyethyleneglycol-coated liposomes into solid tumor tissue by in vivo fluorescence microscopy. Int. J. Pharm. 144, 11–17.

Yamaoka, K., Tanigawa, Y., Nakagawa, T., Uno, T., 1981. A pharmacokinetic analysis program (MULTI) for microcomputer. J. Pharmacobio-Dyn. 4, 879–885.

Yuan, F., Dellian, M., Fukumura, D., Leunig, M., Berk, D.A., Torchilin, V.P., Jain, R.K., 1995. Vascular permeability in a human tumor xenograft: molecular size dependence and cutoff size. Cancer Res. 55, 3752–3756.

International Journal of Pharmaceutics 359 (2008) 272–279

Contents lists available at ScienceDirect

International Journal of Pharmaceutics

journal homepage: www.elsevier.com/locate/ijpharm

Pharmaceutical Nanotechnology

Prolongation of residence time of liposome by surface-modification with mixture of hydrophilic polymers

Tamer Shehata, Ken-ichi Ogawara, Kazutaka Higaki, Toshikiro Kimura*

Department of Pharmaceutics, Faculty of Pharmaceutical Sciences, Okayama University, 1-1-1 Tsushima-naka, Okayama 700-8530, Japan

ARTICLE INFO

Article history:
Received 7 January 2008
Received in revised form 14 March 2008
Accepted 6 April 2008
Available online 12 April 2008

Keywords:
PEG liposome
Polyvinyl alcohol
Pharmacokinetics
Opsonins
Dysopsonins

ABSTRACT

The objective of this study is to evaluate the biodistribution characteristics of liposomes surface-modified with the mixture of polyethylene glycol (PEG) and polyvinyl alcohol (PVA) as a drug carrier for passive targeting of drugs. The liposomes (egg phosphatidylcholine:cholesterol = 55:40, molar ratio) modified with both PEG and PVA (4:1 molar ratio) (PEG4%/PVA1% liposome) provided the largest AUC, which could be attributed to the smallest hepatic clearance of the liposomes. The liver perfusion studies clearly indicated that lower hepatic disposition of PEG4%/PVA1% liposome was ascribed to the decrease in its hepatic uptake via receptor-mediated endocytosis. Furthermore, the amounts of whole serum proteins and of opsonins such as complement C3 and immunoglobulin G adsorbed on PEG4%/PVA1% liposome were significantly smaller than those on the liposome solely modified with PEG (PEG5% liposome). On the other hand, several proteins were adsorbed at larger amount on PEG4%/PVA1% liposome than PEG5% liposome, and the protein identification by LC–MS/MS suggested that some of those proteins including albumin might function as dysopsonins. The decrease in the adsorbed amount of several opsonins and the increase in the adsorbed dysopsonins would be responsible for its lower affinity to the liver and long residence in the systemic circulation of PEG4%/PVA1% liposome.

1. Introduction

Liposomes, mainly made from naturally occurring phospholipids, are biocompatible vehicles. Liposomes can entrap both hydrophilic and hydrophobic drugs in their aqueous internal compartment or within their membrane bilayer, respectively, and hence it can protect the entrapped drug from external destructive condition such as light, pH and enzymes. Therefore, liposomes are considered to be one of the advantageous candidates of drug carriers (Lian and Ho, 2001; Torchilin, 2005). In spite of these merits, their rapid clearance by the reticuloendothelial system (RES) limits their application as drug carriers to other tissues and/or cells (Poste et al., 1982; Senior, 1987; Allen et al., 1991). Various strategies have been developed in order to avoid RES uptake, including the modifying of the liposomal surface with natural polysaccharides such as mannan, pullulan, amylopectin and dextran (Sihorkar and Vyas, 2001). Besides these approaches, long circulating liposomes were developed by the incorporation of ganglioside GM1, phosphatidylinositol or lipid-conjugated polyethylene glycol (PEG) onto the surface (Allen and Chonn, 1987; Gabizon and Papahadjopoulos, 1988; Allen and Hansen, 1991). Among them, many studies have demonstrated that PEG-modified liposome exhibits its prolonged blood circulating property by inhibiting adsorption of various opsonins such as immunoglobulin G (IgG) and complement-related components (Banerjee, 2001; Ishida et al., 2002). PEG liposome has been widely used in an attempt to achieve a passive targeting of drugs due to its easy preparation, relatively low cost and its multiple linkability to other lipids (Allen et al., 1991; Maruyama et al., 1999). Lately, the feasibility of modifying the surface of liposomes with polyvinyl alcohol (PVA) or polyacrylic acid (PAA) having a hydrophobic anchor(s) was reported, and it was confirmed that the modification of the liposomal surface with PVA could improve the physical stability of liposomes (Takeuchi et al., 1998, 2000). In addition, the blood circulation time of PVA (MW: 20,000)-modified liposome was comparable to that of PEG (MW: 2000)-liposome (Takeuchi et al., 2001). However, there has been no report examining the effect of the modification of liposomes with the mixture of different hydrophilic polymers. In order to develop the longer circulating liposomal preparations, therefore, we formulated the liposomes surface-modified with the mixture of PEG and PVA, and evaluated their biodistribution characteristics in rats. The hepatic disposition characteristics of these liposomes were evaluated in the liver perfusion experiments. In addition, to have a better understanding of their in vivo behavior, especially their hepatic uptake, the interaction of these polymer-modified liposomes with blood components was also studied.

* Corresponding author. Tel.: +81 86 251 7948; fax: +81 86 251 7926.
E-mail address: kimura@pharm.okayama-u.ac.jp (T. Kimura).

0378-5173/$ – see front matter © 2008 Elsevier B.V. All rights reserved.
doi:10.1016/j.ijpharm.2008.04.004

2. Materials and methods

2.1. Materials

Egg yolk phosphatidylcholine (EPC), cholesterol (Chol) and distearoyl phosphatidylethanolamine-*N*-[methoxy poly(ethylene glycol)-2000] (PEG-DSPE) were purchased from ASAHI KASEI Chemicals Industry Inc. (Tokyo, Japan), Wako Pure Chemical Industry Inc. (Osaka, Japan) and NOF Inc. (Tokyo), respectively. [^{3}H] Cholesteryl hexadecyl ether ([^{3}H] CHE) was purchased from PerkinElmer Life Science Inc. (Boston, MA, USA). Polyvinyl alcohol derivatives bearing a hydrophobic anchor ($C_{12}H_{25}$–S–) at the terminal of the molecule with molecular weight of 20,000 was a kind gift from Kuraray Co. (Tokyo). Trypsin from porcine pancreas was purchased from Sigma (St. Louis, MO, USA). Calcein was purchased from Kanto Chemical Co. Inc. (Tokyo). Phospholipid content of liposomes was determined using Phospholipid C-Test Wako (Wako Pure Chemical, Osaka). Rabbit anti-rat IgG polyclonal antibody or goat anti-rat complement C3 polyclonal antibody was purchased from Southern Biotech. (Birmingham, AL, USA) or from MP Biomedicals, LLC (Solon, OH, USA), respectively. All other reagents were of the finest grade available.

2.2. Preparation of liposomes

Small unilamellar liposomes were prepared by the hydration method reported previously (Furumoto et al., 2007). PEG2000 is almost completely incorporated into liposomes at 5 mol% of total lipid contents, but its amount incorporated is saturated over 5–7 mol% (Allen et al., 1991). Therefore, we set the total polymer content to be 5 mol%. EPC, Chol and/or PEG-DSPE from stock solution were mixed at the molar ratio of EPC:Chol = 60:40 for conventional liposome or EPC:Chol:polymer(s) = 55:40:5 for polymer-modified liposomes, respectively, the liposomes were radiolabeled by incorporating trace amount of the non-exchangeable, non-metabolizeable marker [^{3}H] CHE to follow the biodistribution of liposomes (Stein et al., 1980). Then, the lipid mixture was dried under reduced pressure. The resultant dried lipid film was hydrated with phosphate-buffered saline (PBS, pH 7.4) under mechanical agitation. The obtained liposomal suspensions were extruded through polycarbonate membrane filters (Millipore, Temecula, CA, USA) with pore sizes of 200 nm 5 times, followed by the extrusion through 100-nm filter 10 times. In order to prepare liposomes-containing PVA, furthermore, an aliquot of the liposomal suspensions were mixed with PVA polymer solution with various concentrations to give an intended final PVA content and was followed by the incubation at 10 °C for 60 min according to the method reported previously (Takeuchi et al., 1998). In the case of calcein-containing liposomes, the hydration of dried lipid film was performed with PBS (pH 7.4) containing calcein (0.2 mg/mL), then the liposomal suspensions were obtained by following the same procedure as described above. Non-encapsulated calcein was removed by gel-filtration chromatography (Sepharose CL-4B, Amersham Bioscience, Uppsala, Sweden). The amount of PVA associated onto the liposomes was estimated by the method reported previously (Takeuchi et al., 1998). In brief, 0.3 mL of liposomal suspension was ultra-centrifuged at 300,000 × *g* for 120 min. The mixture of 3 mL of boric acid solution (4%, w/v) and 0.6 mL of I_2/KI solution (0.05 M/0.15 M) was added to 0.05 mL of the supernatant, then the solution was diluted to 10 mL with distilled water. The polymer concentration was measured spectrophotometrically at the wavelength of 620 nm. The amount of associated PVA was calculated by subtracting the PVA amount in the solution. It was confirmed that more than 90% of added PVA was incorporated into the liposomal membranes.

2.3. Liposomal size distribution and zeta potential measurements

The size distribution and zeta potentials of liposomes in PBS (pH 7.4) were determined by dynamic light scattering spectrophotometer (DLS-7000, Otsuka Electronics, Osaka) and by electrophoretic light scattering spectrophotometer (ELS-6000, Otsuka Electronic), respectively.

2.4. In vitro release of calcein from liposome

The in vitro release of calcein from liposomes was evaluated by equilibrium dialysis method. In brief, 1 mL of liposomal suspension was mixed with 1 mL of PBS (pH 7.4) containing 10% serum (v/v) and the mixture was loaded into the membrane tube (Spectra/Por® Membrane, MWCO: 12,000–14,000, Spectrum Laboratories Inc., Breda, The Netherlands). After both ends were tightly closed, the dialysis tubes were placed into 40 mL of PBS (pH 7.4) as an acceptor medium, and were incubated at 37 °C for 12 h. The percentage of released calcein from liposomes was calculated as follows:

$$\text{release}\,(\%) = \frac{I_r - I_0}{I_{\text{total}} - I_0} \times 100$$

where I_0 and I_r are the fluorescence intensities of calcein before and after incubation, respectively. I_{total} was the florescence intensity of total calcein loaded into liposomes, which was determined after the destabilization of liposomes by 5% Triton X-100 (final concentration). The florescence intensity of calcein was measured at 490 and 520 nm for excitation and emission wavelengths, respectively.

2.5. Animals

Male Wistar rats (Japan SLC, Hamamatsu, Japan), maintained at 25 °C and 55% humidity, were allowed free access to standard laboratory chow (Clear Japan, Tokyo) and water. Rats weighing 220–240 g were randomly assigned to each experimental group. Our investigations were performed after approval by our local ethical committee at Okayama University and in accordance with Principles of Laboratory Animal Care (NIH publication #85-23).

2.6. In vivo disposition experiments

After rats were anesthetized by intraperitoneal injection of sodium pentobarbital (20 mg/kg), liposomes were injected into the femoral vein at a dose of 10 μmol total lipid/kg. Body temperature of rats was kept at 37 °C using a heat lamp during the experiment. Blood samples were withdrawn from the jugular vein at fixed time points, followed by immediate centrifugation at 4000 × *g*. The obtained plasma was collected (100 μL) and scintillation medium (Clear-sol II, Nacalai Tesque, Kyoto) was added. For the tissue distribution study, organs (liver, spleen, kidney, heart and lung) were excised at 6 h after the intravenous injection, rinsed with PBS, and weighed. To solubilize the organs, Soluene-350 (Packard Instrument Inc., Meriden, CT, USA) was added and incubated for 2 h at 50 °C before the solubilized solution was neutralized by HCl. Then, scintillation medium was added to the samples, and radioactivity was measured in a liquid scintillation counter (TRI-CARB® 2260XL, Packard Instrument Inc.).

Plasma concentrations of liposomes (C_p) versus time curves were analyzed by the Eq. (1) using the non-linear least-squares regression program MULTI (Yamaoka et al., 1978).

$$C_p = A \cdot \exp(-\alpha \cdot t) + B \cdot \exp(-\beta \cdot t) \quad (1)$$

The area under the plasma concentration–time curve (AUC) was calculated by the following equation:

$$AUC_0^t = \int_0^t C_p\,dt \tag{2}$$

Total body clearance (CL_{total}), elimination rate constant (k_{el}), distribution volume of central compartment (Vd_c) and distribution volume at steady state (Vd_{ss}) were calculated by the following equations:

$$CL_{total} = \frac{Dose}{AUC_0^\infty} \tag{3}$$

$$Vd_c = \frac{Dose}{A+B} \tag{4}$$

$$k_{el} = \frac{CL_{total}}{Vd_c} \tag{5}$$

$$Vd_{ss} = \left(1 + \frac{k_{12}}{k_{21}} \cdot Vd_c\right) \tag{6}$$

where AUC_0^∞ means AUC value from 0 to infinity. k_{12} and k_{21} are first-order rate constants from peripheral to central compartment and from central to peripheral compartment, respectively. Tissue uptake clearance (CL_{tissue}) was calculated by the following equation:

$$CL_{tissue} = \frac{X_{tissue}^t}{AUC_0^t} \quad (t = 360\,\text{min}) \tag{7}$$

where AUC_0^t means AUC value from 0 to time t and X_{tissue}^t represents the amount of liposomes in a tissue at time t.

2.7. Single-pass liver perfusion experiments

Liver perfusion was carried out following the procedure reported previously (Furumoto et al., 2002). After the liver was stabilized by 13-min perfusion with Krebs–Ringer bicarbonate (KRB) buffer, each liposomal preparation was continuously infused at a concentration of 0.5 nmol total lipid/mL in the presence of 1% serum from the portal vein for 20 min. After 5-min wash with KRB buffer, the liver was excised, weighed and the accumulated amount of liposomes in the liver was evaluated by measuring the radioactivity in the liver as mentioned above. The serum was prepared just before use as follows: rat whole blood was collected from the carotid artery and allowed to clot at room temperature for 20 min, then centrifuged at 1500 × g for 20 min at 4 °C and the supernatant obtained was used. To investigate the contribution of the receptor-mediated endocytosis to the uptake of liposomes, the perfused liver was pretreated with 10 μg/mL trypsin for 10 min (Ogawara et al., 1999).

2.8. Quantitative and qualitative determination of serum protein associated onto liposomal surface

Aliquots of ^{3}H-liposomal suspension (2.5 μmol total lipid/mL) were incubated with equal volume of fresh rat serum for 20 min at 37 °C. Then, the liposomes were separated from bulk serum proteins by Sepharose CL-4B gel filtration (Johnstone et al., 2001). Fractions of liposomes were collected, and the amount of serum proteins associated on liposomes was quantified by Lowry's method (Lowry et al., 1951) and the amount of liposomes was quantified by measuring the radioactivity. SDS-polyacrylamide gel electrophoresis (SDS-PAGE) was performed by using the Mini Protean-II electrophoretic apparatus (Bio-Rad, Hercules, CA, USA) on 12.5% polyacrylamide gel (Ready Gel J, Bio-Rad). For the relative comparison of the proteins associated on the surface of each liposomal preparation, the same amount of protein (0.3 μg) was loaded onto the gel. The detection of proteins was performed by a silver-stain procedure by using a silver-stain kit (Daiichi Pure Chemicals, Tokyo).

After SDS-PAGE was performed as described above, proteins were blotted on cellulose nitrate membrane (Advantec, Tokyo). For the detection of complement C3 or IgG, the blots were incubated with 1:100 diluted goat anti-rat complement C3 or 1:250 diluted rabbit anti-rat IgG polyclonal antibody. As second antibodies, peroxidase-linked anti-goat polyclonal antibody (Cosmo Bio. Tokyo) and anti-rabbit polyclonal antibody (Zymed® laboratories Inc., CA, USA) were used at 1:10,000 and 1:5000 dilution in blocking buffer, respectively. The protein band was visualized with the enhanced chemiluminescence (ECL) system (Amersham Pharmacia Biotech, Buckinghamshire, UK) and the densitometric intensities of protein bands were quantified by Scion Image™ (Scion Corporation, Frederick, MD). Since SDS-PAGE was conducted under reducing condition where many small fragments can be generated from the protein of interest, the densitometric intensities of bands were integrated for each lane to semi-quantitatively evaluate the amount of C3 and IgG.

2.9. Sample preparation for LC–MS/MS analysis and data search

The protein bands were excised from the gel and transferred to Ependorf tubes. The gel pieces were washed twice with 50% acetonitrile/25 mM ammonium bicarbonate, washed with 100% acetonitrile and then dried in a speed vacuum concentration system (CVE-100D, Rikakikai, Tokyo). Approximately 30 μL of trypsin (20 μg/mL) in 25 mM ammonium bicarbonate was added to the dried residue and the samples were incubated overnight at 37 °C. The supernatant was transferred to a separate Ependorf tube and the peptides were further extracted from the gel pieces by incubation in 50% acetonitrile/5% formic acid (FA) for about 4 h at room temperature. The supernatants obtained from the two steps were pooled, dried by SpeedVac and dissolved in 5 μL 50% acetonitrile/0.1% FA and stored at −20 °C until use. Sample analysis was performed on Agilent 1100LC/MSD Trap XCT series system. The ionization system was Chip Cube using HPLC-Chip-Ms (Agilent Technologies, Santa Clara, CA, USA). The chip was automatically loaded and positioned into the MS nanospray chamber. The chip contained a Zobrax 300SB-C_{18} (43 mm × 75 μm, 5 μm) column and a Zobrax 300SB-C_{18} (40 nL, 5 μm) enrichment column. The mobile phase, the mixture of H_2O/0.1% FA and acetonitrile/10% H_2O/0.1% FA, was delivered at the flow rate of 300 nL/min. Tryptic peptides were eluted from the column into the MS using gradient elution. The capillary voltage was set to 1850 V, the flow and temperature of the drying gas were 4 L/min and 300 °C, respectively. The MS and MS/MS data were analyzed by Data Analysis software (Spectrum Mill Ver. 3.3).

2.10. Statistical analysis

Results are expressed as the mean ± S.D. Analysis of variance (ANOVA) was used to test the statistical significance of differences among groups. Statistical significance in the differences of the means was evaluated by using Student's t-test or Tukey's test for the single or multiple comparisons of experimental groups, respectively.

3. Results and discussion

In order to prolong the residence time of liposomes in the systemic circulation, PVA as well as PEG were employed to modify the surface of liposomes. In this study, we prepared five different

Table 1
Composition and physical properties of liposomes

Liposomes	Liposomes composition EPC:Chol:PEG:PVA (molar ratio)	Particle size (nm)	Zeta potential (mV)
Naked	60:40:0:0	90.8 ± 0.9	−29.0 ± 1.2
PEG5%	55:40:5:0	88.5 ± 1.2	−4.5 ± 0.8*
PEG4%/PVA1%	55:40:4:1	91.1 ± 2.1	3.7 ± 0.5
PEG1%/PVA4%	55:40:1:4	124.2 ± 2.2	0.7 ± 0.8
PVA5%	55:40:0:5	141.0 ± 0.6	0.4 ± 1.0

Results for particle size and zeta potential are expressed as the mean ± S.D. of three experiments.
* $p < 0.05$, compared with naked liposome.

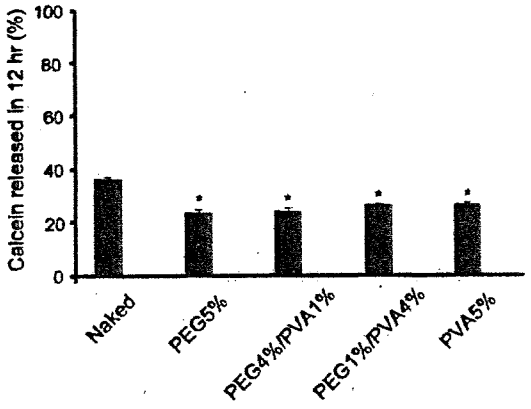

Fig. 1. In vitro release of calcein from surface-modified liposomal preparations. Each liposomal preparation was incubated in PBS (pH 7.4) containing 10% rat serum (v/v) at 37 °C for 12 h. Results are expressed as the mean with the vertical bar showing S.D. of three experiments. * $p < 0.05$, compared with naked liposome.

liposomal preparations including naked liposome, PEG liposome (PEG5%), liposomes modified with the mixture of both PEG and PVA (PEG4%/PVA1% and PEG1%/PVA4%) and liposome modified with PVA only (PVA5%). It is well known that PEG-DSPE is stably inserted into the lipid bilayer of liposomes (Parr et al., 1994). The 1-h incubation with 50% rat serum at 37 °C revealed that more than 90% of PVA incorporated stably remained on the liposomes, suggesting that the hydrophobic moiety of PVA derivative was also stably inserted into the lipid bilayer of liposomes as suggested by Takeuchi et al. (1998).

Since several factors such as particle size, charge and lipid composition have been reported to influence the in vivo fate of liposomes after intravenous administrations (Levchenko et al., 2002; Murao et al., 2002; Awasthi et al., 2003), the physicochemical properties of the liposomes prepared were examined (Table 1). The particle sizes for naked and PEG liposomes were found to be almost the same, while the modification of liposomes with PVA increased the particle size depending on its molar ratio. The measurement of zeta potential showed that the negative charge of naked liposome tended to be neutralized by the surface-modification either

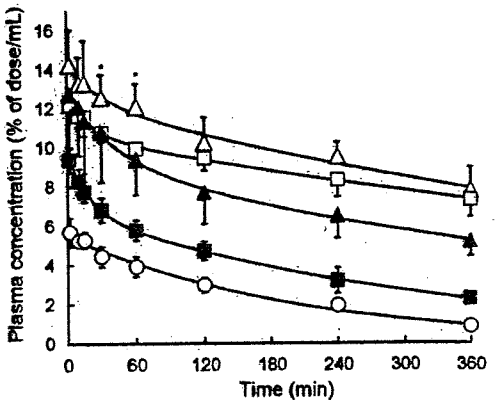

Fig. 2. Plasma concentration–time profile of surface-modified liposomal preparations after intravenous injection into rats. Each liposomal preparation was injected at a dose of 10 μmol total lipid/kg. Results are expressed as the mean with the vertical bar showing S.D. of three rats. Keys: –○–, Naked; –□–, PEG5%; –△–, PEG4%/PVA1%; –▲–, PEG1%/PVA4%; –■–, PVA5%. * $p < 0.05$ compared with PEG5% liposome.

with PEG, PVA or their mixture. In order to confirm the stability of prepared liposomes in the presence of serum, calcein release from each liposomal preparation was determined. As illustrated in Fig. 1, the surface-modified liposomes were characterized by the significant lower release of calcein compared to the naked liposome, demonstrating their good stability in the presence of serum.

In vivo pharmacokinetics and biodistribution of the surface-modified liposomes were investigated after intravenous administration to rats. Fig. 2 shows the plasma concentration–time profiles of the liposomes, and the pharmacokinetic parameters obtained are summarized in Table 2. As shown in Fig. 2, naked liposome was rapidly eliminated from systemic circulation with the largest values of k_{el}, Vd_c and Vd_{ss} (Table 2). On the other hand, other polymer-modified liposomes exhibited longer blood circulating properties. Among them, PEG4%/PVA1% liposome showed the smallest CL_{total} and the largest AUC_0^∞, which was about 12 times or 1.2 times larger than that of naked liposome or PEG5% liposome, respectively (Table 2). In addition, the PEG4%/PVA1% liposome showed significantly higher plasma levels than PEG5% liposome at 30 and 60 min after intravenous injection. Moreover, the PEG4%/PVA1% liposome provided the smallest values of both Vd_c and k_{el} among the liposomal preparations examined, where the small Vd_c and k_{el} would mean the decrease in the rapid distribution to the liver just after dosing and the delay of elimination from plasma, respectively. Tissue uptake clearances calculated for various organs would support the above consideration (Fig. 3). The hepatic clearances for the liposomes modified with polymers were significantly smaller than that for naked liposome, and PEG4%/PVA1% liposome provided the smallest value of hepatic clearance among the liposomes investigated. Furthermore, it is worth to note that PEG4%/PVA1% liposome showed significantly smaller clearances for liver (68%), spleen (38%) and lung (22% of PEG5%) than PEG5% liposome. On the other hand,

Table 2
Pharmacokinetic parameters of different liposomal formulations after intravenous injection into rats

Parameters	Naked	PEG5%	PEG4%/PVA1%	PEG1%/PVA4%	PVA5%
AUC (% of dose min/mL)	1096 ± 101	10755 ± 3012**	13438 ± 4520**	6045 ± 604	2267 ± 282
CL_{total} (μL/min)	91.9 ± 8.3	9.7 ± 2.4**	8.0 ± 2.4**	16.7 ± 1.6**	44.6 ± 5.3**
k_{el} (min^{-1})	4.98 ± 0.24	1.21 ± 0.36**	1.13 ± 0.36**	2.12 ± 0.25**	4.29 ± 0.42
Vd_c (mL)	18.4 ± 1.1	8.1 ± 0.5**	7.1 ± 0.9**	8.0 ± 1.7**	10.4 ± 0.7**
Vd_{ss} (mL)	18.4 ± 1.1	9.4 ± 0.3**	9.5 ± 2.3**	10.6 ± 2.3**	14.3 ± 1.4

Each pharmacokinetic parameter was obtained by following the equations described in Section 2. Results are expressed as the mean ± S.D. of three rats.
** $p < 0.01$, compared with naked liposome.

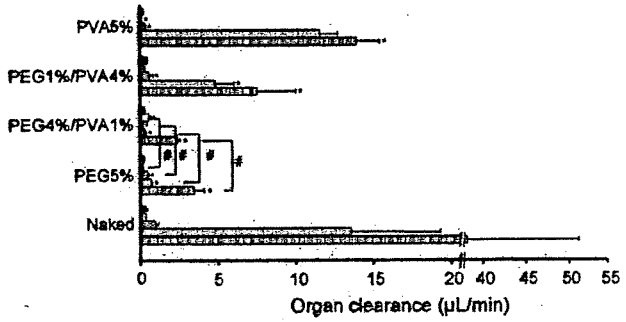

Fig. 3. Tissue uptake clearances of surface-modified liposomes after intravenous injection into rats. Each liposomal preparation was injected at a dose of 10 μmol total lipid/kg. Each tissue was excised at 6 h after injection. Results are expressed as the mean with the vertical bar showing S.D. of three rats. Keys: ▨, liver; ▨, spleen; ▨, lung; □, kidney; ■, heart. $^{*}p<0.05$ compared with naked liposome; $^{\#}p<0.05$ compared with PEG5% liposome.

the renal uptake clearance was larger for PEG4%/PVA1% liposome than that for PEG5% liposome. The reason for it remains to be clarified, but the longer circulation of larger amount of liposomes might lead to the disposition of intact and/or degraded liposomes into kidney.

To clarify the mechanism behind the less affinity of PEG4%/PVA1% than PEG5% to the liver where these liposomes were mainly distributed, a single-pass liver perfusion experiment was performed by using the perfusate containing 1% serum (v/v) (Fig. 4). Naked liposome showed significantly higher hepatic accumulation (4.3 ± 1.2 nmol total lipid) than the two polymer-modified liposomes. In addition, the hepatic accumulation of PEG4%/PVA1% liposome (0.6 ± 0.2 nmol total lipid) was significantly lower than PEG5% (1.9 ± 0.3 nmol total lipid). These results were similar to those obtained in the in vivo study (Figs. 2 and 3 and Table 2). Furthermore, the pretreatment of the perfused liver with trypsin drastically decreased the hepatic accumulation of both naked (0.96 ± 0.1 nmol total lipid) and PEG5% liposomes (0.90 ± 0.06 nmol total lipid). On the contrary, the same treatment did not significantly affect the hepatic accumulation of PEG4%/PVA1% liposome (0.70 ± 0.20 nmol total lipid). These results clearly indicate that the modification of liposomes with the mixture of PEG4%/PVA1% can avoid the hepatic disposition via the receptor-mediated endocytosis, which, on the other hand, substantially contributes to the hepatic disposition of PEG5% liposome.

It is well known that the hepatic uptake of liposomes is largely affected by the association of serum opsonins such as IgG,

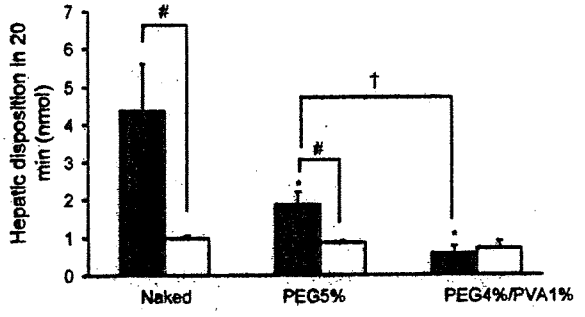

Fig. 4. Hepatic disposition of naked, PEG5% and PEG4%/PVA1% liposomes in single-pass liver perfusion experiments. The liver perfusion was performed for 20 min. Results are expressed as the mean with the vertical bar showing S.D. of three experiments. Keys: ■, control; □, + trypsin treatment. $^{*,\#,\dagger}p<0.05$, compared with naked, control or PEG5% liposome, respectively.

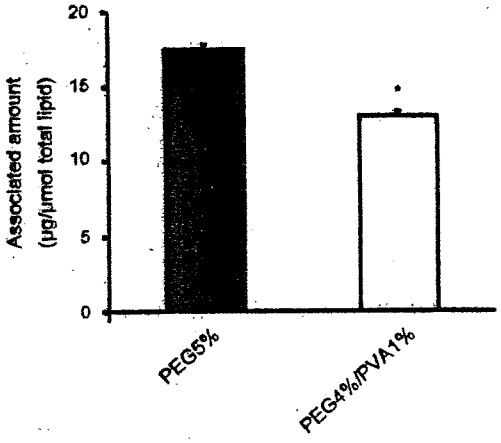

Fig. 5. Amount of serum proteins associated on the surface of PEG5% and PEG4%/PVA1% liposomes. Results are expressed as the mean with the vertical bar showing S.D. of three experiments. $^{*}p<0.05$, compared with PEG5% liposome.

fibronectin, complement components, C-reactive protein and α_2-macroglobulin (Tsujimoto et al., 1981; Rossi and Wallace, 1983; Bonte and Juliano, 1986; Huong et al., 2001; Price et al., 2001; Ishida et al., 2006; Moghimi et al., 2006). In addition, the recognition of surface-bound opsonins by their corresponding receptors is known to be a main trigger for the hepatic uptake of particles via receptor-mediated endocytosis (Moghimi and Davis, 1994; Liu et al., 1995). Therefore, we tried to evaluate the serum proteins associated on the surface of PEG5% liposome and PEG4%/PVA1% liposome quantitatively and qualitatively. As illustrated in Fig. 5, the total amount of serum proteins adsorbed on the surface of the PEG4%/PVA1% liposome (13.0 ± 0.3 μg/μmol total lipid) was significantly smaller than that for PEG5% liposome (18.0 ± 0.4 μg/μmol total lipid). This result was in good agreement with the previous report demonstrating that the circulation half-lives of liposomes after intravenous administration is inversely related to the total protein amount associated on the surface (Chonn et al., 1992). It has previously been reported that the fixed aqueous layer thickness (FALT) around liposomes was increased by the surface-modification with PEG and that thicker FALT would be likely to prevent serum proteins from interacting with liposomes (Shimada et al., 1995; Zeisig et al., 1996). Moreover, it has been postulated that surface-grafted PEG would form either a mushroom or a brush conformation, depending on molecular weight and surface density of PEG on the liposomes, and that the latter conformation would build the thicker FALT than the former one (Needham et al., 1997; Nicholas et al., 2000; Johnstone et al., 2001). Sadzuka et al. (2002) reported that the surface-modification with the mixture of PEG500 and PEG2000 provided thicker FALT than the modification with either PEG500 or PEG2000, and that the liposomes modified with both PEG500 and PEG2000 revealed the lowest hepatic uptake. They speculated that PEG500 would facilitate to transform of PEG2000 from the mushroom structure into the brush one, and that the liposomes on which less amount of opsonins would be adsorbed due to thicker FALT had lower affinity to the liver (Sadzuka et al., 2002). Considering this background, we speculated that PVA alone on the surface of liposomes would be present as the mushroom (shrunk) structure with thin FALT. Then, further addition of adequate amount of PEG might facilitate the conformational change of PVA to the brush-like (extended) structure with thicker FALT, leading to the decrease in the adsorbed amount of serum proteins on PEG4%/PVA1% liposome. In the case of PEG1%/PVA4% liposome, the amount of PEG might be still insufficient to facilitate the conformation change of PVA. Sadzuka et

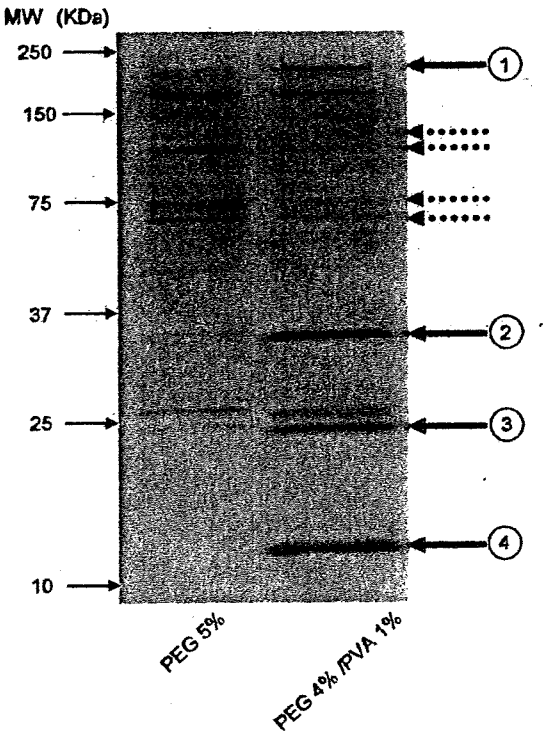

Fig. 6. Comparison of serum proteins associated on the surface of PEG5% and PEG4%/PVA1% liposomes. The same amount of protein (0.3 μg) was loaded onto each lane. SDS-PAGE was performed following the procedure described in Section 2, and proteins were silver-stained. Solid and dotted arrows indicate the typical proteins increased and decreased on PEG4%/PVA1% liposome, respectively, as compared with PEG5% liposome.

al. (2002) proposed that the optimal amount of PEG500 would be needed to support the brush-like structure of PEG2000 and it could also be the case with PEG/PVA liposomes. To have better understanding of the mechanisms; however, the conformational dynamics of PVA molecule on the surface have to be elucidated and will be the subject of our further study.

In order to identify the proteins adsorbed on the liposomes, SDS-PAGE was at first performed. The results revealed that there was quite large difference in the profiles of surface-associated serum proteins between PEG5% liposome and PEG4%/PVA1% liposome (Fig. 6). The proteins highlighted with dotted arrows seem to be preferentially associated onto PEG5% liposome. On the other hand, the proteins highlighted with solid arrows (15, 25, 35 and 240 kDa) are associated more onto PEG4%/PVA1% liposome. Taken the results obtained in the in vivo and liver perfusion studies together, the proteins with dotted arrows might contain opsonins enhancing the hepatic uptake of PEG5% liposome, while the proteins with solid arrows might possess dysopsonin-like activity suppressing the uptake of PEG4%/PVA1% liposome.

As discussed above, complement C3 (C3) and IgG are the major opsonins and are known to play important roles to promote the hepatic uptake of liposomes via their corresponding receptors expressed on the surface of Kupffer cells in the liver (Ishida et al., 2002). Therefore, we conducted the Western blot analysis to compare the amounts of C3 and IgG associated on the surface of PEG5% and PEG4%/PVA1% liposomes (Fig. 7). As shown in Fig. 7A and B, the semi-quantification of the densitometric intensities derived from C3 and IgG fragments revealed that these typical opsonins associated more with PEG5% liposome than PEG4%/PVA1% liposome.

Besides opsonins, it has been suggested that there are some dysopsonins in serum, which can inhibit phagocytosis of pathogens or particles. Although it was reported that immunoglobulin A and α_1-acid glycoprotein functioned as dysopsonins for microorganisms (Van Oss et al., 1974; Absolom, 1986), there is no identified serum components with dysopsonic activity for liposomes so far. Then, we tried to identify the proteins which might act as dysopsonin for PEG4%/PVA1%, highlighted with solid arrows in Fig. 6. After SDS-PAGE was performed for proteins associated on PEG4%/PVA1% liposome, the proteins highlighted with solid arrows in Fig. 6 were subjected to LC–MS/MS system for identification and the results were summarized in Table 3. The analysis showed that albumin would be one of the serum proteins preferentially associated onto PEG4%/PVA1% liposome. Taken our previous reports that the pre-coating of polystyrene nanospheres with albumin or the coupling of albumin onto the surface of PEG liposome reduced their affinity to the liver (Ogawara et al., 2004; Furumoto et al., 2007), albumin might function as dysopsonin for PEG4%/PVA1% liposome.

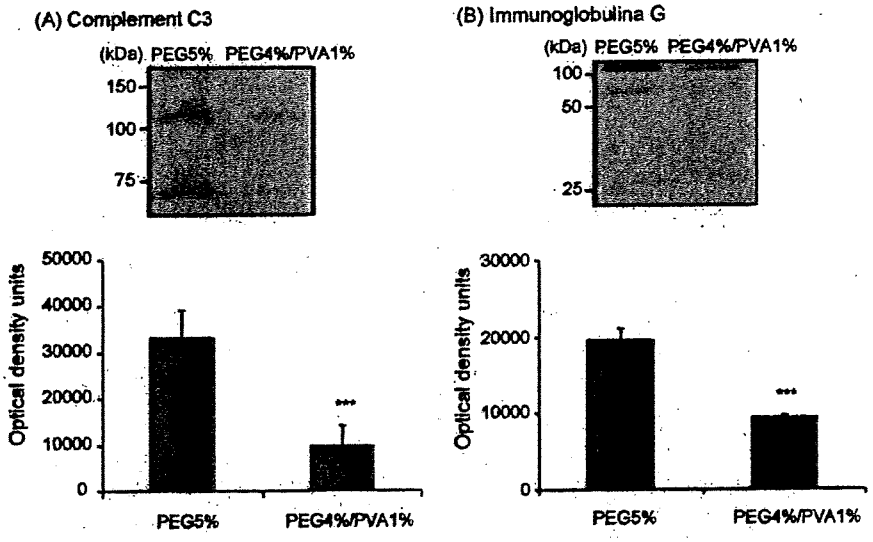

Fig. 7. Semi-quantification of complement C3 and immunoglobulin G associated on the surface of PEG5% and PEG4%/PVA1% liposomes by Western blot analysis. The same amount of protein (1.2 μg) was loaded onto each lane. Results of semi-quantification are expressed as the mean with the bar showing S.D. of five experiments. $^{***}p < 0.05$ compared with PEG5% liposomes.

Table 3
Identification of several serum proteins associated on PEG4%/PVA1% liposome at larger amount than PEG5% liposomes

Band number	Identified proteins	Accession number	Spectrum Mill score
1	Apolipoprotein B	61098031	43.67
2	Apolipoprotein A-IV	8392909	96.62
	Albumin	55391508	41.07
3	Apolipoprotein E	37805241	186.39
4	Apolipoprotein A-I	113997	97.65
	Albumin		

LC–MS/MS data were analyzed by Spectrum Mill with NCBInr database (http://www.ncbi.nlm.nih.gov/). The following filters were used after database searching: peptide score >6, peptide% SPI > 60 and protein score > 11. Band numbers represent the proteins highlighted with solid arrows in Fig. 6.

In addition, apo A-I, A-IV, B and E were also shown to preferentially be associated onto PEG4%/PVA1% liposome. Although apoE itself is known to function as an opsonin for the uptake of particles by hepatocytes, Bisgaier et al. (1989) indicated that the co-existence of apoE with apoA-I, A-IV or B leads to the conformational change of apoE and abolishes its ability to enhance the uptake of liposomes by HepG2 cells. Therefore, the enrichment of these apolipoproteins on the surface of PEG4%/PVA1% liposome might abolish the opsonic activity of apoE. However, the mechanisms by which the specific proteins such as albumin, apo A-I, A-IV, B and E were preferentially associated onto PEG4%/PVA1% liposome are still unclear and would be investigated in the further study.

4. Conclusion

An incorporation of small percentage of PVA into PEG liposome (PEG4%/PVA1% liposome) improved the in vivo disposition characteristics, which could be attributed to lower hepatic distribution of PEG4%/PVA1% liposome. The decrease in the affinity to the liver would be attributed to lower amount of serum proteins including opsonins and larger amount of dysopsonins such as albumin adsorbed on the surface. These findings can form a solid basis to develop useful particulate drug carriers with better in vivo disposition characteristics. To confirm the advantage of PEG4%/PVA1% liposome, the in vivo anti-tumor activity of the liposome including some anti-tumor drug will be investigated in our next study.

References

Absolom, D.R., 1986. Opsonins and dysopsonins: an overview. Methods Enzymol. 132, 281–318.

Allen, T.M., Chonn, A., 1987. Large unilamellar liposomes with low uptake into the reticuloendothelial system. FEBS Lett. 223, 42–46.

Allen, T.M., Hansen, C., 1991. Pharmacokinetics of stealth versus conventional liposomes: effect of dose. Biochim. Biophys. Acta 1068, 133–141.

Allen, T.M., Hansen, C., Martin, F., Redemann, C., Yau-Young, A., 1991. Liposomes containing synthetic lipid derivatives of poly(ethylene glycol) show prolonged circulation half-lives in vivo. Biochim. Biophys. Acta 1066, 29–36.

Awasthi, V.D., Garcia, D., Goins, B.A., Phillips, W.T., 2003. Circulation and biodistribution profiles of long-circulating PEG-liposomes of various sizes in rabbits. Int. J. Pharm. 253, 121–132.

Banerjee, R., 2001. Liposomes: applications in medicine. J. Biomater. Appl. 16, 3–21.

Bisgaier, C.L., Siebenkas, M.V., Williams, K.J., 1989. Effects of apolipoproteins A-IV and A-I on the uptake of phospholipid liposomes by hepatocytes. J. Biol. Chem. 264, 862–866.

Bonte, F., Juliano, R.L., 1986. Interactions of liposomes with serum proteins. Chem. Phys. Lipids 40, 359–372.

Chonn, A., Semple, S.C., Cullis, P.R., 1992. Association of blood proteins with large unilamellar liposomes in vivo: relation to circulation lifetimes. J. Biol. Chem. 267, 18759–18765.

Furumoto, K., Ogawara, K., Nagayama, S., Takakura, Y., Hashida, M., Higaki, K., Kimura, T., 2002. Important role of serum proteins associated on the surface of particles in their hepatic disposition. J. Control. Rel. 83, 89–96.

Furumoto, K., Yokoe, J., Ogawara, K., Amano, S., Takaguchi, M., Higaki, K., Kai, T., Kimura, T., 2007. Effect of coupling of albumin onto surface of PEG liposome on its in vivo disposition. Int. J. Pharm. 329, 110–116.

Gabizon, A., Papahadjopoulos, D., 1988. Liposome formulations with prolonged circulation time in blood and enhanced uptake by tumors. Proc. Natl. Acad. Sci. U.S.A. 85, 6949–6953.

Huong, T.M., Ishida, T., Harashima, H., Kiwada, H., 2001. Species difference in correlation between in vivo/in vitro liposome-complement interactions. Biol. Pharm. Bull. 24, 439–441.

Ishida, T., Harashima, H., Kiwada, H., 2002. Liposome clearance. Biosci. Rep. 22, 197–224.

Ishida, T., Ichihara, M., Wang, X., Yamamoto, K., Kimura, J., Majima, E., Kiwada, H., 2006. Injection of PEGylated liposomes in rats elicits PEG-specific IgM, which is responsible for rapid elimination of a second dose of PEGylated liposomes. J. Control. Rel. 112, 15–25.

Johnstone, S.A., Masin, D., Mayer, L., Bally, M.B., 2001. Surface-associated serum proteins inhibit the uptake of phosphatidylserine and poly (ethylene glycol) liposomes by mouse macrophages. Biochim. Biophys. Acta 1513, 25–37.

Levchenko, T.S., Rammohan, R., Lukyanov, A.N., Whiteman, K.R., Torchilin, V.P., 2002. Liposome clearance in mice: the effect of a separate and combined presence of surface charge and polymer coating. Int. J. Pharm. 240, 95–102.

Lian, T., Ho, R., 2001. Trends and development in liposome drug delivery systems. J. Pharm. Sci. 90, 667–680.

Liu, D., Liu, F., Song, Y.K., 1995. Recognition and clearance of liposomes containing phosphatidylserine are mediated by serum opsonin. Biochim. Biophys. Acta 1235, 140–146.

Lowry, O.H., Rosebrough, N.J., Farr, A.L., Randall, R.J., 1951. Protein measurement with the Folin phenol reagent. J. Biol. Chem. 1951, 265–275.

Maruyama, K., Ishida, O., Takizawa, T., Moribe, K., 1999. Possibility of active targeting to tumor tissues with liposomes. Adv. Drug Deliv. Rev. 40, 89–102.

Moghimi, S.M., Davis, S.S., 1994. Innovations in avoiding particle clearance from blood by Kupffer cells: cause for reflection. Crit. Rev. Ther. Drug Carrier Syst. 11, 31–59.

Moghimi, S.M., Hamad, I., Bunger, R., Andresen, T.L., Jorgensen, K., Hunter, A.C., Baranji, L., Rosivall, L., Szebeni, J., 2006. Activation of the human complement system by cholesterol-rich and PEGylated liposomes-modulation of cholesterol-rich liposome-mediated complement activation by elevated serum LDL and HDL levels. J. Liposome Res. 16, 167–174.

Murao, A., Nishikawa, M., Managit, C., Wong, J., Kawakami, S., Yamashita, F., Hashida, M., 2002. Targeting efficiency of galactosylated liposomes to hepatocytes in vivo: effect of lipid composition. Pharm. Res. 19, 1808–1814.

Needham, D., Stoicheva, N., Zhelev, D.V., 1997. Exchange of monooleoylphosphatidylcholine as monomer and micelle with membranes containing poly(ethylene glycol)–lipid. Biophys. J. 73, 2615–2629.

Nicholas, A.R., Scott, M.J., Kennedy, N.I., Jones, M.N., 2000. Effect of grafted polyethylene glycol (PEG) on the size, encapsulation efficiency and permeability of vesicles. Biochim. Biophys. Acta 1463, 167–178.

Ogawara, K., Furumoto, K., Nagayama, S., Minato, K., Higaki, K., Kai, T., Kimura, T., 2004. Pre-coating with serum albumin reduces receptor-mediated hepatic disposition of polystyrene nanosphere: implications for rational design of nanoparticles. J. Control. Rel. 100, 451–455.

Ogawara, K., Yoshida, M., Takakura, Y., Hashida, M., Higaki, K., Kimura, T., 1999. Interaction of polystyrene microspheres with liver cells: role of membrane receptors and serum proteins. Biochim. Biophys. Acta 1472, 165–172.

Parr, M.J., Ansell, S.M., Choi, L.S., Cullis, P.R., 1994. Factors influencing the retention and chemical stability of poly(ethyleneglycol)–lipid conjugates incorporated into large unilamellar vesicles. Biochim. Biophys. Acta 1195, 21–30.

Poste, G., Bucana, C., Raz, A., Bugelski, P., Kirsh, R., Fidler, I.J., 1982. Analysis of the fate of systemically administered liposomes and implications for their use in drug delivery. Cancer Res. 42, 1412–1422.

Price, M.E., Cornelius, R.M., Brash, J.L., 2001. Protein adsorption to polyethylene glycol modified liposomes from fibrinogen solution and from plasma. Biochim. Biophys. Acta 1512, 191–205.

Rossi, J.D., Wallace, B.A., 1983. Binding of fibronectin to phospholipid vesicles. J. Biol. Chem. 258, 3327–3331.

Sadzuka, Y., Nakade, A., Hirama, R., Miyagishima, A., Nozawa, Y., Hirota, S., Sonobe, T., 2002. Effect of mixed polyethyleneglycol modification on fixed aqueous layer thickness and antitumor activity of doxorubicin containing liposome. Int. J. Pharm. 238, 171–180.

Senior, J.H., 1987. Fate and behavior of liposomes in vivo: a review of controlling factors. Crit. Rev. Ther. Drug Carrier Syst. 3, 123–193.

Shimada, K., Miyagishima, A., Sadzuka, Y., Nozawa, Y., Mochizuki, Y., Ohshima, H., Hirota, S., 1995. Determination of the thickness of the fixed aqueous layer around polyethyleneglycol-coated liposomes. J. Drug Target 3, 283–289.

Sihorkar, V., Vyas, S.P., 2001. Potential of polysaccharide anchored liposomes in drug delivery, targeting and immunization. J. Pharm. Pharm. Sci. 4, 138–158.

Stein, Y., Halperin, G., Stein, O., 1980. Biological stability of [^{3}H] cholesteryl oleyl ether in cultured fibroblasts and intact rat. FEBS Lett. 111, 104–106.

Takeuchi, H., Kojima, H., Yamamoto, H., Kawashima, Y., 2000. Polymer coating of liposomes with a modified polyvinyl alcohol and their systemic circulation and RES uptake in rats. J. Control. Rel. 68, 195–205.

Takeuchi, H., Kojima, H., Yamamoto, H., Kawashima, Y., 2001. Evaluation of circulation profiles of liposomes coated with hydrophilic polymers having different molecular weights in rats. J. Control. Rel. 75, 83–91.

Takeuchi, H., Yamamoto, H., Toyoda, T., Toyobuku, H., Hino, T., Kawashima, Y., 1998. Physical stability of size controlled small unilamellar liposomes coated with a modified polyvinyl alcohol. Int. J. Pharm. 164, 103–111.

Torchilin, V.P., 2005. Recent advances with liposomes as pharmaceutical carriers. Nat. Rev. Drug Discov. 4, 145–160.
Tsujimoto, M., Inoue, K., Nojima, S., 1981. Reactivity of human C-reactive protein with positively charged liposomes. J. Biochem. (Tokyo) 90, 1507–1514.
Van Oss, C.J., Gillman, C.F., Bronson, P.M., Border, J.R., 1974. Phagocytosis-inhibiting properties of human serum alpha-1 acid glycoprotein. Immunol. Commun. 3, 321–328.
Yamaoka, K., Nakagawa, T., Uno, T., 1978. Statistical moments in pharmacokinetics. J. Pharmacokinet. Biopharm. 6, 547–558.
Zeisig, R., Shimada, K., Hirota, S., Arndt, D., 1996. Effect of sterical stabilization on macrophage uptake in vitro and on thickness of the fixed aqueous layer of liposomes made from alkylphosphocholines. Biochim. Biophys. Acta 1285, 237–245.

Volume 49, Issue 2, February 2008 ISSN 0923-1811

JOURNAL OF DERMATOLOGICAL SCIENCE

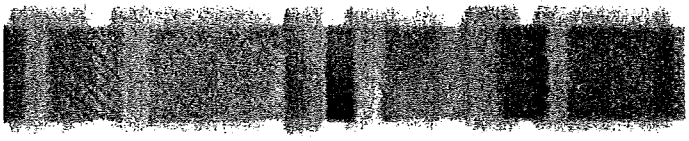

The official journal of The Japanese Society for Investigative Dermatology

Available online at ScienceDirect www.sciencedirect.com

Journal of Dermatological Science (2008) 49, 174–177

Journal of Dermatological SCIENCE

www.intl.elsevierhealth.com/journals/jods

LETTER TO THE EDITOR

ATX-S10(Na)-photodynamic therapy inhibits cytokine secretion and proliferation of lymphocytes

KEYWORDS
ATX-S10(Na); HuT102 cells; IFN-γ; IL-6; IL-8; TNF-α

Photodynamic therapy (PDT) is a new therapeutic modality for a variety of neoplasms, including skin tumors, lymphomas, as well as scleroderma. Now PDT using 5-aminolevulinic acid (ALA) is available for skin diseases and its effects on cytokine production have also been reported [1,2]. ATX-S10(Na),13,17-bis(1-carboxypropionyl)carbamoylethyl-8-ethenyl-2-hydroxy-3-hydroxyiminoethylidene-2,7,12,18-tetramethylporphyrin sodium salt, is a new hydrophilic chlorine photosensitizer characterized by good accumulation in tumors [3,4], and rapid elimination in urine within 24–48 h. Thus ATX-S10(Na) is regarded as a good candidate for the second generation photosensitizer of PDT. Recent study from our laboratory has demonstrated that ATX-S10(Na)-PDT is effective for various skin tumors [5].

Psoriasis is a chronic inflammatory skin disease with hyperproliferative epidermis. It is assumed that T cells and various T cell-derived cytokines reveal an essential role on induction and maintenance of the psoriatic lesion [6]. In fact cyclosporine and various biological agents are effective for psoriasis. There are no reports, however, which describe the effect of PDT on cytokine production or T cell proliferation. In the present study, we investigated the effect of ATX-S10(Na)-PDT on the production of cytokines and viability of various T cell lines.

These cell lines include HuT102, MT-2, Jurkat, MoLT4, which are derived from mycosis fungoides, adult T cell leukemia, acute lymphoblastic leukemia, and acute lymphoblastic leukemia, respectively. These were generous gifts from Dr. Hiroya Kobayashi (Pathology, Asahikawa Medical College, Japan). The cells were cultured in RPMI 1640 medium containing 10% fetal calf serum, 100 u/ml penicillin, and 100 μg/ml streptomycin at 37 °C in CO_2 in air. In order to determine the production of cytokines, 10^6 cells were cultured for 24 h and supernatants were collected. Then various cytokines, TNF-α, IFN-γ, IL-2, IL-5, IL-6, and IL-8, were assayed using ELISA kits, which were purchased from BioSource International, Inc. (California, USA). In a preliminary study, HuT102 cells produced abundant cytokines, such as TNF-α, IFN-γ, IL-6, and IL-8, but not IL-2, or IL-5 (data not shown). Then we analyzed the effect of ATX-S10(Na)-PDT on the cytokine production of HuT102 cells.

HuT102 cells (1×10^6) were cultured in the presence of 10 μg/ml ATX-S10(Na) for 3 h and the cells were washed with phosphate-buffered saline (PBS). Then the cells were irradiated with diode laser (LD670-05, Hamamatsu Photonics K.K, Hamamatsu, Japan). At the indicated time the supernatants were collected and cytokine assays were performed. ATX-S10(Na)-PDT significantly inhibited TNF-α, IFN-γ, IL-6, and IL-8 production and the maximal effect was observed at 24 h (Fig. 1). The effect was irradiation dose-dependent. ATX-S10(Na) or the laser irradiation alone did not affect the cytokine secretions or cell proliferation (data not shown). Similar inhibitory effects on the cytokines production were observed by ATX-S10(Na)-PDT using MT-2, Jurkat, and MoLT4 cells (data not shown).

The effect of ATX-S10(Na)-PDT on cell proliferation was performed by non-radioactive proliferation assay using tetrazolium as indicator (Promega, Madison, WI). Various doses of laser were irradiated on 1×10^6 HuT102 cells, which were pretreated by 10 μg/ml ATX-S10(Na) for 3 h. The decrease in cell proliferation was observed at 6 h and the maximal effect was detected at 24 h (data not shown). The suppressive effect was detected at 40 mJ/cm^2 with dose-dependent inhibition up to 100 mJ/cm^2

Abbreviations: PBS, phosphate-buffered saline; PDT, photodynamic therapy.

doi:10.1016/j.jdermsci.2007.07.015

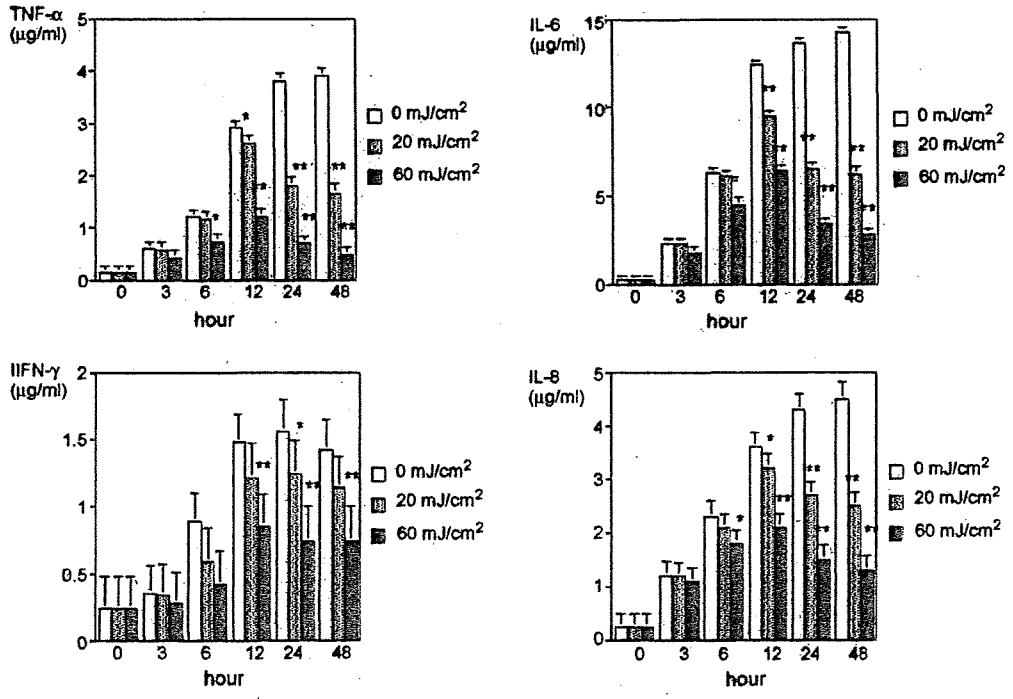

Fig. 1 Effect of ATX-S10(Na)-PDT on cytokine secretion of HuT102 cells. Following ATX-S10(Na)-PDT, supernatants of cultured HuT102 cells were collected at the indicated time and TNF-α, IFN-γ, IL-6, and IL-8 assays were performed. Data are the means ± S.E.M. from triplicate determinations of at least four independent experiments. $^{*}P < 0.05$ compared with 0 mJ/cm^2; $^{**}P < 0.01$ compared with 0 mJ/cm^2.

(Fig. 2A). The effect of ATX-S10(Na)-PDT on cell death was performed by counting viable cells using 0.5% trypan blue. The cell death was detected at 40 mJ/cm^2 with dose-dependent inhibition up to 100 mJ/cm^2 (Fig. 2A). The dead cells showed nuclear condensation and bleb, the features of apoptosis (data not shown). Similar inhibitory effects were observed using MT-2, Jurkat, and MoLT4 cells (data not shown).

The present study demonstrated that ATX-S10(Na)-PDT suppressed cytokine secretion from T lymphocytes. High dose irradiation (60 mJ/cm^2) suppressed cytokine secretion associated with decreased cell proliferation. In contrast, low dose irradiation (20 mJ/cm^2) suppressed cytokine secretion without the inhibition of cell proliferation. PDT induces singlet oxygen, which results in cell death by oxidative damage on cell membranes and

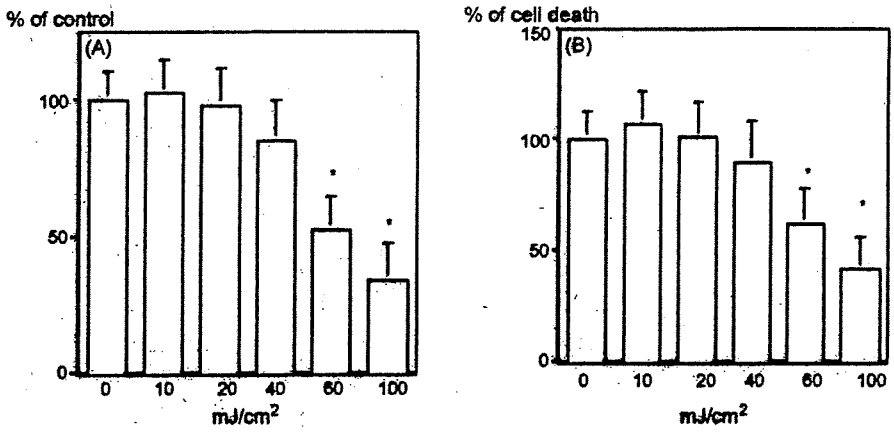

Fig. 2 Effect of ATX-S10(Na)-PDT on cell proliferation and cell death of HuT102 cells. After ATX-S10(Na)-PDT, HuT102 cells were cultured for 24 and then MTS assay (A) and counting number of dead cells which were stained by trypan blue (B) were performed. Data are the means ± S.E.M. from triplicate determinations of at least four independent experiments. $^{*}P < 0.01$ compared with 0 mJ/cm^2.

mitochondria [7]. Our preliminary study disclosed that 60 mJ/cm^2 irradiation induced apoptosis in HuT102 cell. Thus the suppression of cytokine secretion by PDT at high dose irradiation was most likely due to the cell death. Kick et al. [8] demonstrated that IL-6 expression in PDT-treated HeLa cells is modulated by AP-1. They also showed that PDT-induced AP-1 activation is mediated by H_2O_2 and antioxidants indicating redox-dependent regulation. Previous study revealed that AP-1 activation by redox signal inhibits IL-2 gene expression [9]. The suppression of cytokines by PDT with low dose irradiation might be mediated by redox-regulated transcriptional factors, such as AP-1, and NF-κB.

Previous reports showed the effect of PDT on cytokine production. Consistent with our results, PDT using photofrin suppressed TNF-α and IL-8 production in lymphocytes derived from psoriasis patients [2]. In contrast, PDT using photofrin induced TNF-α, IL-6, IL-8, and IL-10 production in epithelial cells, mammary tumor cells, HeLa cells, and macrophages [1]. These results indicate that the effect of PDT on cytokine production depends on different tissues and/or photosensitizers.

The cytotoxic effect of ATX-S10(Na)-PDT on lymphoid cells was also demonstrated in the present study, which may explain the effect of PDT on cutaneous lymphoma [9]. It is well known that electron beam is among the first line therapies for the early stage cutaneous lymphoma. Because cutaneous lymphomas such as mycosis fungoides require long-term treatments, several adverse effects including radiation dermatitis, bone marrow suppression, and potential secondary carcinogenesis might be expected. Because the cytotoxic effect of ATX-S10(Na)-PDT was much less than that of the electron beam treatment, ATX-S10(Na)-PDT might be another useful modality for the treatment of cutaneous lymphomas, in which the electron beam treatment is restricted by the maximal irradiation dose and the resting time interval for the next irradiation.

Psoriasis is an inflammatory skin disease accompanied with hyperproliferative epidermis and increased microvessels in the upper dermis. It is presumed that a variety of cytokines, such as, TNF-α, IFN-γ, IL-6, and IL-8, are involved in the pathogenesis of psoriasis [6]. Our study demonstrated that these cytokines from lymphocytes was suppressed by ATX-S10(Na)-PDT. PDT using photofrin or ALA has been clinically applied for the treatment of psoriasis [10]. ATX-S10(Na)-PDT-induced suppression of cytokine production as well as lymphocyte cytotoxicity at higher dose might be promising for its clinical use against psoriasis.

In summary, we have shown that ATX-S10(Na)-PDT suppresses cytokine secretion of various lymphocyte cell lines. These results might provide a clue for the new treatment modality for psoriasis, cutaneous lymphomas, and other related skin disorders.

References

[1] Evans S, Matthews W, Perry R, Fraker D, Norton J, Pass HI. Effect of photodynamic therapy on tumor necrosis factor production by murine macrophages. J Nat Cancer Inst 1990;82:34–9.

[2] Boehcke WH, Konig K, Kaufmann R, Scheffold W, Prümmer O, Sterry W. Photodynamic therapy in psoriasis: suppression of cytokine production in vitro and recording of fluorescence modification during treatment in vivo. Arch Dermatol Res 1994;286:300–3.

[3] Nakajima S, Sakata I, Takemura T. Tumor localizing and photosensitization of photo-chlorin ATX-S10(Na). In: Spinelli P, dal Fante M, Marchesini R, editors. Photodynamic therapy and biological lasers. Amsterdam: Elsevier; 1992. p. 531–4.

[4] Nakajima S, Sakata I, Hirano T, Takemura T. Therapeutic effect of interstitial photodynamic therapy using ATX-S10(Na) and a diode laser on radio-resistant SCC II tumors of C3H/He mice. Anticancer Drugs 1998;9:539–43.

[5] Takahashi H, Itoh Y, Nakajima S, Sakata I, Iizuka H. ATX-S10(Na) photodynamic therapy for human skin tumors and benign hyperproliferative skin. Photodermatol Photoimmunol Photomed 2004;20:257–65.

[6] Kennedy JP, Pottier RH, Pross DC. Photodynamic therapy with endogenous protoporphyrin IX: basic principles and present clinical experience. J Photochem Photobiol B 1990;6:143–8.

[7] Griffiths CEM. The immunological basis of psoriasis. J Eur Acad Dermatol Venererol 2003;17(Suppl. 2):1–5.

[8] Kick G, Messer G, Goetz A, Plewig G, Kind P. Photodynamic therapy induces expression of interleukin 6 by activation of AP-1 but not NF-κB DNA binding. Cancer Res 1995;55: 2373–9.

[9] Beiqing L, Chen M, Whisler RL. Sublethal levels of oxidative stress stimulate transcriptional activation of c-jun and suppress IL-2 activation in Jurkat T cells. J Immunol 1996;157: 160–9.

[10] Gad F, Viau G, Boushira, Bertrand R, Bissonnette R. Photodynamic therapy with 5-aminolevulinic acid induces apoptosis and caspase activation in malignant T cells. J Cut Med Surg 2001;5:8–13.

Hidetoshi Takahashi*
Akemi Ishida-Yamamoto
Department of Dermatology, Asahikawa Medical College, 2-1-1-1 Midorigaokahigashi, Asahikawa 078-8510, Japan

Susumu Nakajima
Photochemical Research Division, Moriyama Memorial Hospital, Asahikawa 078-8510, Japan

Isao Sakata
Photochemical Co. Ltd., 5319-1 Haga, Okayama 701-1221, Japan

Hajime Iizuka
Department of Dermatology, Asahikawa Medical College, 2-1-1-1 Midorigaokahigashi, Asahikawa 078-8510, Japan

*Corresponding author. Tel.: +81 166 65 2111; fax: +81 166 68 2529
E-mail address: ht@asahikawa-med.ac.jp (H. Takahashi)

7 April 2007

Clin Orthop Relat Res (2008) 466:1726–1733
DOI 10.1007/s11999-008-0284-6

ORIGINAL ARTICLE

Photodynamic Therapy with ATX-S10·Na(II) Inhibits Synovial Sarcoma Cell Growth

Ken Takeda MD, Toshiyuki Kunisada MD, PhD, Shinichi Miyazawa MD, PhD, Yoshinori Nakae, Toshifumi Ozaki MD, PhD

Received: 30 September 2007 / Accepted: 22 April 2008 / Published online: 9 May 2008

Abstract Photodynamic therapy (PDT) is an effective cancer treatment modality that allows selective destruction of malignant tumor cells. We asked whether PDT could inhibit in vivo and in vitro growth of synovial sarcoma cells. We analyzed PDT using ATX-S10·Na(II) and a diode laser for a synovial sarcoma cell line (SYO-1). Photodynamic therapy with ATX-S10·Na(II) showed an in vitro cytotoxic effect on the cultured SYO-1 cells. The in vitro effect of PDT depended on the treatment concentration of ATX-S10·Na(II) and the laser dose of irradiation. ATX-S10·Na(II) was detected in the tumor tissue specimens that were excised from nude mice bearing SYO-1 within 6 hours after intravenous injection, but it was eliminated from the tumor 12 hours after injection. Photodynamic therapy suppressed the tumor growth of nude mice bearing SYO-1, and high-dose irradiation induced no viable tumor cells in histologic specimens. Photodynamic therapy performed after marginal resection of the tumor of nude mice bearing SYO-1 reduced the rate of local recurrence of the tumor. Our results suggest PDT using ATX-S10·Na(II) and laser irradiation may be a potentially useful treatment for synovial sarcoma, especially to reduce the surgical margin and preserve critical anatomic structures adjacent to the tumor.

One or more of the authors (TK, TO) have received funding from Grants-in-aid for Young Scientists (B) from the Ministry of Education, Culture, Sports, Science and Technology (18791040 and 15790792), by a grant from the Japan Orthopaedics and Traumatology Foundation Inc (0158), by Grants-in-Aid for Clinical Cancer Research and Grants-in-Aid for Cancer Research (14S-4 and -5) from the Ministry of Health, Labor and Welfare, and by a grant from the JSPS Fujita Memorial Fund for Medical Research.
Each author certifies that his or her institution has approved the animal protocol for this investigation and that all investigations were conducted in conformity with ethical principles of research.

K. Takeda, S. Miyazawa, T. Ozaki
Department of Orthopaedic Surgery, Science of Functional Recovery and Reconstruction, Okayama University Graduate School of Medicine, Dentistry, and Pharmaceutical Sciences, Okayama, Japan

T. Kunisada (✉)
Department of Medical Materials for Musculoskeletal Reconstruction, Okayama University Graduate School of Medicine, Dentistry, and Pharmaceutical Sciences, 2-5-1, Shikata-cho, Okayama 700-8558, Japan
e-mail: toshi-kunisada@umin.ac.jp

Y. Nakae
Photochemical Co, Ltd, Okayama, Japan

Introduction

Photodynamic therapy is a unique cancer treatment modality based on the dye-sensitized photooxidation of biologic matter in target tissue [25, 26]. An intravenous injection of a light-sensitive agent (the photosensitizer) is retained selectively by tumor cells. The photosensitizer can be focally excited by laser light in the presence of oxygen using light of a wavelength matched to an absorption peak of the photosensitizer [3], and it transfers energy from photons to oxygen molecules. Direct killing of tumor cells, vascular damage, and inflammatory responses contribute to tumor destruction [2, 7]. Photodynamic therapy, with systemic administration of photosensitizer and laser irradiation, has been used clinically in recent years. It has advantages such as anatomic and functional preservation of adjacent normal tissues, enabling minimally invasive procedures and adjuvant therapy for unresectable cancers [16, 29, 31]. Various authors report PDT has an antitumor effect

in lung [10, 18], esophageal [8], bladder [1, 12], and dermatologic cancers [24, 33]. Photodynamic therapy also has been used to treat noncancerous diseases such as choroidal neovascularization [22], atherosclerosis [30], and benign hyperproliferative skin [28].

Malignant musculoskeletal tumors typically require wide surgical resection with normal surrounding tissue. However, a wide surgical resection often results in poor physical function postoperatively according to the amount of excised normal tissue, including muscle, vessels, and nerves. Preservation of such normal surrounding tissue can lead to better postoperative function for the patient, although there is a higher risk of local recurrence. Adjuvant treatment may reduce the risk of local recurrence when decreasing the surgical margin. The effect of chemotherapy and radiotherapy remains controversial regarding musculoskeletal tumors [4, 6, 32]. Photodynamic therapy could be a novel adjuvant treatment for musculoskeletal tumors. Several papers report the treatment of osteosarcoma with acridine orange PDT and chondrosarcoma with BPD PDT [5, 13, 14].

ATX-S10·Na(II) is one of the hydrophilic chlorine photosensitizers and has some advantages compared with other photosensitizers. ATX-S10·Na(II) can be eliminated rapidly from normal tissue, usually within 48 hours after injection, thus resulting in reduced skin photosensitization [27]. Its absorption maximum lies at 670 nm, which allows deeper penetration of laser beams into tissues than a 630-nm laser [19]. Photodynamic therapy with ATX-S10·Na(II) can be more effective for treatment of deeply located or large tumors, but has not been explored for use in soft tissue sarcomas.

Exploring the possibility that PDT using ATX-S10·Na(II) could be a new therapy for synovial sarcoma we asked four questions: (1) Does PDT have a cytotoxic effect on human synovial sarcoma cells in vitro?; (2) Can ATX-S10·Na(II) accumulate specifically in the tumor after intravenous injection in vivo, and be eliminated from the tumor quickly?; (3) Can PDT using ATX-S10·Na(II) and laser irradiation cause tumor necrosis and inhibit tumor progression?; and (4) Can PDT using ATX-S10·Na(II) and laser irradiation reduce the rate of local recurrence after marginal resection of synovial sarcoma? In this study, we conducted in vivo and in vitro experiments using a human synovial sarcoma cell line to assess these questions.

Materials and Methods

To answer these four questions we conducted four series of experiments (Fig. 1). To assess an in vitro cytotoxic effect of PDT, we measured the cell viability of synovial sarcoma cells after PDT using laser irradiation (10–50 J/cm^2) following incubation with ATX-S10·Na(II) (3.25–50 μg/mL) for 24 hours. To assess the in vivo accumulation of ATX-S10·Na(II) in the tumor, we performed fluorescence microscopic examination of the tumor xenograft of synovial sarcoma cells on nude mice after an intravenous

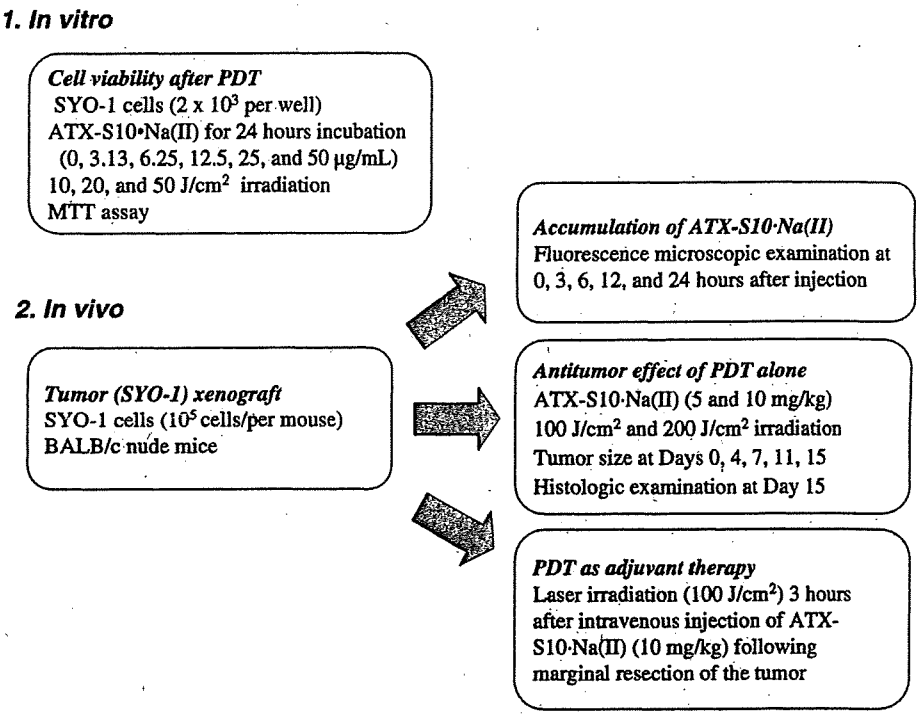

Fig. 1 The diagram shows the experiments we performed for observation of in vitro and in vivo antitumor effects on synovial sarcoma.

injection of ATX-S10·Na(II) (10 mg/kg) during a course of 0 to 24 hours. To assess the efficacy of PDT on the tumor in vivo, we measured the size of the tumor xenograft on nude mice for 15 days after PDT treatment with laser irradiation (100, 200 J/cm^2) following intravenous injection of ATX-S10·Na(II) (5, 10 mg/kg). Because the maximal laser penetration depth was reported as less than 8 mm [17], PDT was performed when the diameter of the tumor xenograft on the nude mice was 5.5 mm. The size of each treated tumor (five mice for each group) at Day 15 after PDT was compared with the size of the untreated control tumors (five mice). Histologic examination of the tumor xenograft was performed on Day 15 after PDT. To answer the question of PDT reducing local recurrence of the tumor, we compared the rates of local recurrence after marginal resection followed by PDT with a 10 mg/kg injection of ATX-S10·Na(II) and 100 J/cm^2 laser irradiation, or after marginal resection alone (five mice in each group). In all experiments, the concentration of ATX-S10·Na(II) and the dose of laser irradiation were not randomized.

ATX-S10·Na(II),13,17-bis(1,2-dicarboxyethyl)carbamoyl ethyl-8-ethenyl-2-hydroxy-3-hydroxyiminoethylidene-2,7, 12,18-tetramethylporphyrin sodium salt was synthesized by a commercial laboratory (Photochemical Co, Ltd, Okayama, Japan). We dissolved ATX-S10·Na(II) in phosphate-buffered saline, and diluted in a culture medium at appropriate concentrations. A diode laser, ALD-1 (Hamamatsu Photonics KK, Hamamatsu, Japan), was used as the light source to excite ATX-S10·Na(II). The diode laser is a continuous-wave laser and its wavelength is 670 nm.

A human synovial sarcoma cell line, SYO-1 [11], was incubated in Dulbecco's modified Eagle's medium supplemented with 10% fetal bovine serum and antibiotics (penicillin and streptomycin) in a humidified atmosphere with 5% CO_2 at 37°C.

We incubated SYO-1 cells (2×10^3 per well) in a 96-well microplate with 0, 3.13, 6.25, 12.5, 25, and 50 μg/mL ATX-S10·Na(II) for 24 hours. The cells were washed with medium twice and then irradiated with 10, 20, and 50 J/cm^2 using the 670-nm diode laser. The laser power was fixed at 150 mW/cm^2. After additional 24-hour incubation of the cells at 37°C, cell viability was assessed by an MTT assay (Chemicon International, Inc, Temecula, CA). Quantitation then was measured using a Model 550 microplate reader (BioRad, Hercules, CA). We prepared eight wells for each condition and the cytotoxicity rate in treated cells was represented as a percentage of MTT value, and compared with that of untreated control cells.

Fifty 4-week-old male BALB/c nude mice (BALB/c nu/nu) were used for implantation of SYO-1 cells. We injected single cell suspensions of SYO-1 cells (10^5 cells per mouse) subcutaneously into the back of the mice. Growth of the tumors was measured using a slide caliper. When the diameter of the tumor reached 10 mm (1.5–2 weeks), ATX-S10·Na(II) (10 mg/kg) was injected intravenously into five SYO-1-bearing mice. The tumors were removed at 0, 3, 6, 12, and 24 hours after injection, respectively. Four frozen sections of the tumor were embedded in OCT compound and prepared for fluorescence microscopy coupled with a cooled CCD camera (Axioplan 2 Imaging; Carl Zeiss, Inc, Thornwood, NJ). A 5-μm unstained frozen section was excited by 520 nm light, and the fluorescence of ATX-S10·Na(II) was examined under a 585-nm band pass filter by the CCD camera.

When the diameter of the tumor on the back of the nude mice reached 5.5 mm, ATX-S10·Na(II) (5 and 10 mg/kg) was injected intravenously. We irradiated the tumor site with 670 nm laser light (100 J/cm^2, 200 J/cm^2) 3 hours after injection (five mice for each group). The duration of PDT was related to the laser dose (11 minutes for 100 J/cm^2 and 22 minutes for 200 J/cm^2). After PDT, the animals were maintained in a dark room to avoid skin irritation. The length and width of the tumors were measured at Days 0, 4, 7, 11, 15 after laser irradiation and then tumor volume was calculated by using the equation: tumor volume (mm^3) = [maximum diameter (mm)][minimum diameter (mm)]^2/2. The mice were euthanized by an intraperitoneal injection of a barbiturate (120 mg/kg) on Day 15 after PDT. Tumor specimens excised from mice were fixed with 4% PFA and embedded in paraffin before undergoing microscopic examinations. Slides of the 4-μm-thick specimens were stained with hematoxylin and eosin. All sections were viewed by two (TK, SM) individuals who were blind to results. Results did not differ between observers.

We examined the efficacy of PDT as an adjuvant treatment to reduce surgical margins, such as for marginal resections of a tumor, without excising surrounding normal tissue. It might be difficult to treat tumors that are large or deeply localized with PDT alone owing to limitations in laser penetration. After the diameter of the tumor on the back of the mice was 12 mm, a marginal resection of the tumor on mice bearing SYO-1 was performed 3 hours after intravenous injection of ATX-S10·Na(II). We divided the mice into two groups: (1) marginal resection without PDT (control), which means resection of the tumor without excision of the surrounding normal tissue; and (2) marginal resection followed by PDT with 100 J/cm^2 laser irradiation 3 hours after intravenous injection of 10 mg/kg ATX-S10·Na(II) ($n = 10$ for each group). The mice were observed until 8 weeks after marginal resection of the tumors.

Each continuous variable of the tumor volume resulting from PDT to the tumor xenograft was expressed as

mean + SD. A nonparametric Mann-Whitney U test was used to compare the tumor volume on Day 15 after PDT with each condition (5 and 10 mg/kg ATX-S10·Na(II) and 100 J/cm^2 and 200 J/cm^2 laser irradiation) with tumor volume of the untreated control group. We compared the rate of tumor recurrence after marginal resection of the xenograft with or without PDT using Fisher's exact probability test. Taking into account our power analysis, we considered a probability value less than 5% as significant throughout the study. All statistical analyses were performed using Stat View 5.0 software (SAS Institute Inc, Cary, NC).

Results

MTT assay revealed PDT using ATX-S10·Na(II) had a cytotoxic effect on and inhibited the growth of SYO-1 cells in vitro. The cytotoxic effect of PDT on SYO-1 cells was dependent on the ATX-S10·Na(II) concentration and the level of laser irradiation (Fig. 2). A higher dose of laser irradiation induced a strong antitumor effect under each concentration of ATX-S10·Na(II). No antitumor effect was observed in the SYO-1 cells treated with laser irradiation without ATX-S10·Na(II) and also with the exposure to ATX-S10·Na(II) without laser irradiation. Photodynamic therapy inhibited tumor growth of SYO-1-bearing mice by Day 15 compared with the untreated control group (ATX-S10·Na(II) 5 mg/kg and laser 100 J/cm^2, $p = 0.047$; 10 mg/kg and 100 J/cm^2, $p = 0.021$; 5 mg/kg and 200 J/cm^2, $p = 0.007$; and 10 mg/kg and 200 J/cm^2, $p = 0.007$) (Fig. 3). The tumors had disappeared completely 4 days after injections of 5 and 10 mg/kg ATX-S10·Na(II) and laser irradiation with 200 J/cm^2. Regrowth of the tumor was not observed until 15 days after PDT under such conditions. However, the tumor was growing gradually after PDT with injections of 5 and 10 mg/kg ATX-S10·Na(II) and laser irradiation with 100 J/cm^2. Injection of ATX-S10·Na(II) without irradiation or laser irradiation without injection of ATX-S10·Na(II) did not inhibit tumor growth.

ATX-S10·Na(II) accumulated into the tumor xenograft of SYO-1 cell on nude mice after the intravenous injection. A marked fluorescence of ATX-S10·Na(II) was observed in the tumor excised from SYO-1-bearing mice 3 and 6 hours after intravenous injection of ATX-S10·Na(II) (Fig. 4). The fluorescence of ATX-S10·Na(II) in the tumor was minimally evident 12 and 24 hours after injection of ATX-S10·Na(II). ATX-S10·Na(II) injected intravenously was incorporated into the SYO-1 forming tumor and thereafter remained inside the tumor for at least 6 hours. ATX-S10·Na(II) was almost totally eliminated from the tumor within the next 6 hours.

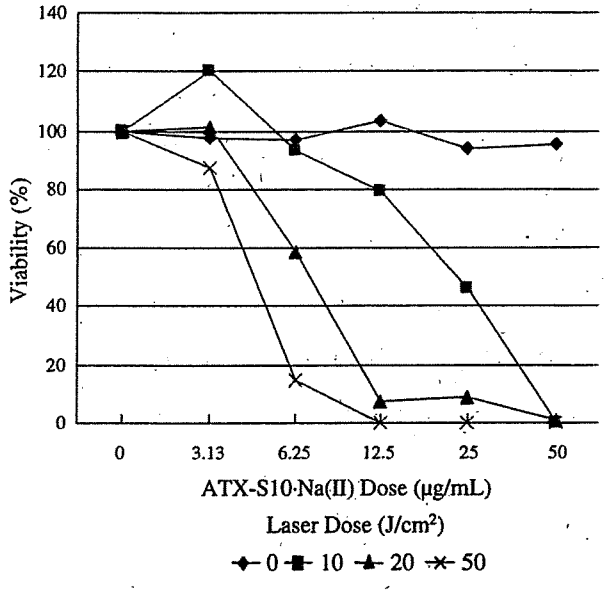

Fig. 2 An MTT assay showed an in vitro antitumor effect of PDT using ATX-S10 Na(II) with a diode laser on SYO-1 cells. The cells were incubated with 0 to 50 μg/mL ATX-S10 Na(II) at 37°C for 24 hours before 670-nm diode laser radiation with 0 to 50 J/cm^2. The cytotoxicity rate in the treated cells is represented as a percentage of MTT value and in comparison to that of the untreated control cells. Higher dye concentrations and laser irradiation levels induced an antitumor effect in a dose-dependent manner.

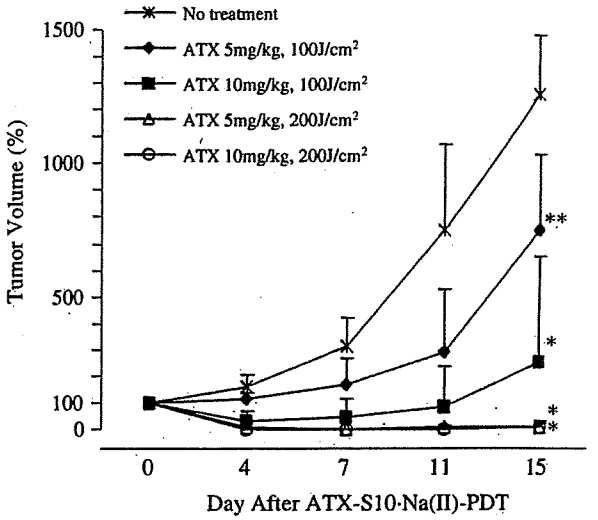

Fig. 3 The tumor growth of SYO-1-bearing mice after ATX-S10·Na(II) PDT is shown. Tumor growth was inhibited (*$p < 0.01$, **$p < 0.05$) within 15 days after PDT with 5 and 10 mg/kg ATX-S10·Na(II) and 100 and 200 J/cm^2 laser irradiation. No tumor regrowth was seen within 15 days after PDT with 5 and 10 mg/kg ATX-S10·Na(II) and 200 J/cm^2 laser irradiation. The data are represented as mean + standard deviation.

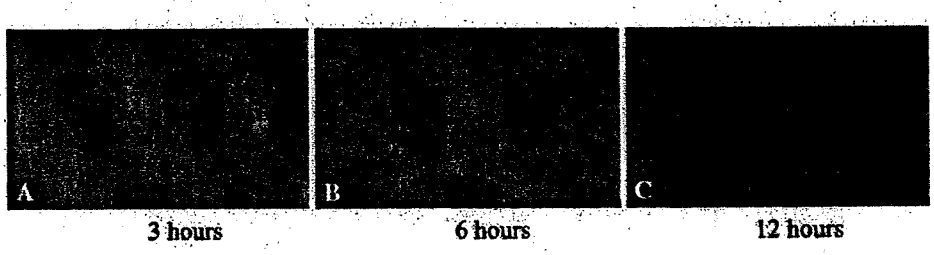

Fig. 4A–C The illustrations show microscopic distribution of ATX-S10·Na(II) fluorescence in SYO-1-forming tumors on nude mice at (A) 3 hours, (B) 6 hours, and (C) 12 hours after intravenous injection of ATX-S10·Na(II). A marked fluorescence of ATX-S10·Na(II) was observed in the tumor resected from SYO-1-bearing mice at (A) 3 and (B) 6 hours after the intravenous injection of ATX-S10·Na(II), but was not observed at (C) 12 hours after injection.

The tumor was growing on Days 11 and 15 after PDT with injection of 5 mg/kg ATX-S10·Na(II) and laser irradiation of 100 J/cm^2 (Fig. 5A), but was not observed macroscopically on Day 15 after PDT with 10 mg/kg ATX-S10·Na(II) and 100 J/cm^2 laser irradiation (Fig. 5B) and with 10 mg/kg ATX-S10·Na(II) and 100 J/cm^2 laser irradiation (Fig. 5C). No necrotic areas were observed inside the tumors on Day 15 after PDT with injection of 5 mg/kg ATX-S10·Na(II) and irradiation with 100 J/cm^2 (Fig. 5D, E). Photodynamic therapy with injection of 10 mg/kg ATX-S10·Na(II) and irradiation with 100 J/cm^2 caused partial necrosis of the tumor in the mice. However, an area of viable tumor cells remained under the necrotic area (Fig. 5F, G). With PDT with injections with 5 and 10 mg/kg ATX-S10·Na(II) and irradiation with 200 J/cm^2, necrotic tissue without viable tumor cells was seen in the entire tumor area (Fig. 5H, I). Histologic analysis of the skin overlying a tumor showed a normal structure in all of the PDT-treated mice 15 days after treatment.

Photodynamic therapy substantially suppressed local recurrence after marginal resection of the tumor. Nine of 10 mice had local recurrence within 8 weeks after marginal resection of the tumor without PDT. Two of 10 mice had local recurrence after marginal resection of the tumor followed by PDT (Table 1). No side effects, such as delayed wound healing or skin defects, were evident with PDT with marginal resection (Fig. 6). None of the mice experienced walking disability until 8 weeks after PDT. The rate of local recurrence after marginal resection followed by PDT was lower ($p = 0.006$) than that after marginal resection only. Local tumor recurrence occurred in the peripheral area of PDT.

Discussion

Limb salvage surgery is considered the standard procedure for soft tissue sarcoma such as synovial sarcoma. Wide resection of the tumor with the surrounding normal tissue is necessary to prevent local recurrence for limb salvage surgery. A curative surgical margin sometimes requires excision of the surrounding normal tissue, such as the nerves, vessels, and muscles with tumor, that sometimes leads to poor postoperative limb function. Therefore, reduction of the surgical margin such as preservation of major vessels and nerves could result in better postoperative function. However, this might increase the risk of local tumor recurrence. In searching for better adjuvant therapy, we explored the possibility that photodynamic therapy using ATX-S10·Na(II) could be a novel therapy for synovial sarcoma. We asked whether PDT with ATX-S10·Na(II) could have an in vitro cytotoxic effect on synovial sarcoma cells, whether ATX-S10·Na(II) accumulated in the tumor in vivo, whether PDT could inhibit tumor progression in nude mice, and whether PDT could suppress local tumor recurrence after marginal resection.

Our study has several limitations. The major limitations of our investigation are limited penetration depth of laser light and skin photosensitization after PDT. Because soft tissue sarcomas, such as a synovial sarcoma, often occur in deep layers of soft tissue, the tumor should not be treated only with PDT. We believe PDT can be applied to the surrounding tissue after tumor resection as an adjuvant therapy to reduce the surgical margin. Photodynamic therapy after tumor resection also may result in less skin complications. Various studies on PDT using ATX-S10·Na(II) have been reported, but ATX-S10·Na(II) has not been studied for clinical use in humans. No data are available regarding clinical complications or toxicities caused by PDT using ATX-S10·Na(II). According to some studies, major complications or toxicities were not observed by the injection of ATX-S10·Na(II) into experimental animals [20, 27, 28]. The lethal dose of ATX-S10·Na(II) for a rat seems to be approximately 1000 mg/kg (personal communication, Dr. Isao Sakata, December 26, 2007).

Patients treated with PDT using Photofrin stayed in a dark room for approximately 1 week after treatment because of hyperphotosensitivity of the skin induced by the photosensitizer [20]. ATX-S10·Na(II) was developed as a novel hydrophilic chlorine photosensitizer that was rapidly eliminated from normal tissues after injection, thus